Evaluation of acute abdominal conditions by Computed Tomography

e-Poster: P-233

Congress: ESGAR 2008

Type: Educational Exhibit

Topic: Diagnostic / Liver / Other / Acute and Post-Traumatic Abdomen

Authors: L. Curvo-Semedo, J.F. Costa, J. Brito, A. Canelas, B.J.A.M. Gonçalves, M.F.S. Seco, B. Graça, A. Costa, F. Caseiro-Alves; Coimbra/PT

MeSH:

Abdomen, Acute [C23.888.646.100.200]

Abdomen, Acute [C23.888.821.030.249]

Tomography, Spiral Computed [E01.370.350.350.810.800]

Keywords: Computed tomography, Acute abdomen

1. Learning objectives

To adress the advantages and drawbacks of Computed Tomography (CT) in the study of acute abdominal conditions.

To illustrate several diagnoses readily apparent on CT and to show some common mimickers.

2. Background

Acute abdomen is defined as a clinical syndrome characterized by sudden onset of severe abdominal pain requiring emergency medical or surgical treatment.

A small number of conditions is however responsible for over 56% of the cases of acute abdomen, the most frequent being acute appendicitis (28%), acute cholecystitis (10%) and small bowel obstruction (4%). In about one-third of the patients, even after surgery, no diagnosis could be reached.

In these patients, a prompt and accurate diagnosis is essential in order to minimize morbidity and mortality, but the clinical presentation of many entities frequently overlaps, and the physical and laboratory examinations are often non-specific.

As a result the diagnosis can be quite challenging, and computed tomography (CT) has become the first-line imaging modality in patients with acute abdominal pain, since it consistently proved to be a time-effective and accurate imaging method, also yielding alternative diagnoses to the main clinical suspicion in some cases.

This method is superior to plain radiography in several settings:

- -In confirming the diagnosis in the majority of patients
- -In revealing the site and cause of a small bowel obstruction (SBO)
- -In detecting a small pneumoperitoneum
- -In identifying urinary stones

In comparison to ultrasonography, CT has the important advantage of not being compromised by bowel gas and fat, which may be a decisive issue when studying patients with acute abdominal conditions.

In particular, the multi-detector CT technology brought various advantages which contributed decisively to the pivotal role that CT possesses today:

- – Shorter acquisition time, leading to less motion and respiratory artefacts
- – Thinner collimation, allowing sub-millimetre isotropic imaging, with resultant high-quality 2D and 3D reformats and reconstructions
- – Better contrast exploitation, permitting separation of multiple enhancement phases

The study protocol should be adapted to the clinical-laboratorial findings of each patient. It is generally useful to acquire non-enhanced images, since they may be needed to depict areas of haemorrhage or calcified stones. Nevertheless, non-enhanced studies alone can be extremely difficult to interpret and the use of contrast agents is usually required. Intra-venous iodinated contrast agents are useful in the majority of situations, and, except when there is suspicion of a vascular condition (which warrants the acquisition of images during the arterial phase), images obtained during the portal venous phase are generally sufficient to reach a diagnosis in most situations. An oral contrast

agent may be used when a GI tract perforation is likely; however, it needs some times to opacify bowel and it may obscure stones haemorrhage or ischemia. Regarding rectal contrast, it is today considered that there is no sufficient benefit to warrant its use.

3. Imaging findings OR Procedure details

Acute pain can be classified according to its topographic location: right upper quadrant (RUQ), left upper quadrant (LUQ), left lower quadrant (LLQ), right lower quadrant (RLQ), epigastric, generalized or flank pain.

The most relevant clinical condition causing RUQ pain is acute cholecystitis (Fig.1).

slide1.jpg

CT findings of acute cholecystitis include (Fig.2):

- -Wall thickening > 3 mm
- -Distended gallbladder
- -Peri-cholecystic fluid
- -Haziness of peri-cholecystic fat
- -Increased attenuation of bile
- -THAD of adjacent liver
- -Intra-mural or intra-luminal gas (emphysematous cholecystitis)
- -Complications (Fig.3)
- - – Perforation
  - – Peri-cholecystic abscess

slide2.jpg

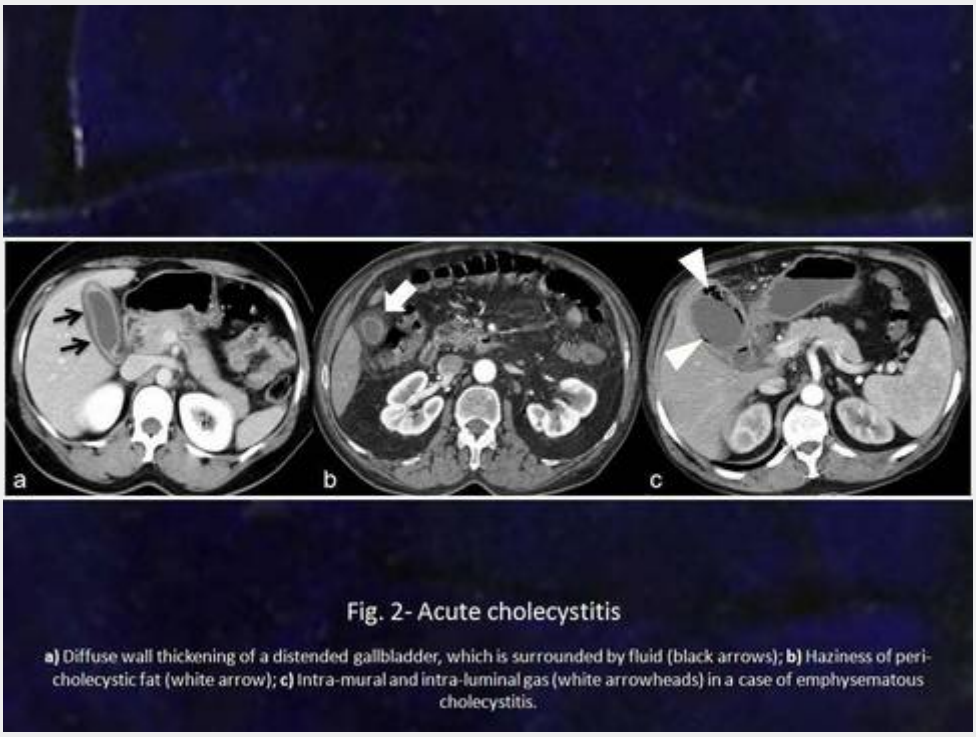

Fig. 2- Acute cholecystitis

a) Diffuse wall thickening of a distended gallbladder, which is surrounded by fluid (black arrows); **b)** Haziness of peri-cholecystic fat (white arrow); **c)** Intra-mural and intra-luminal gas (white arrowheads) in a case of emphysematous cholecystitis.

slide3.jpg

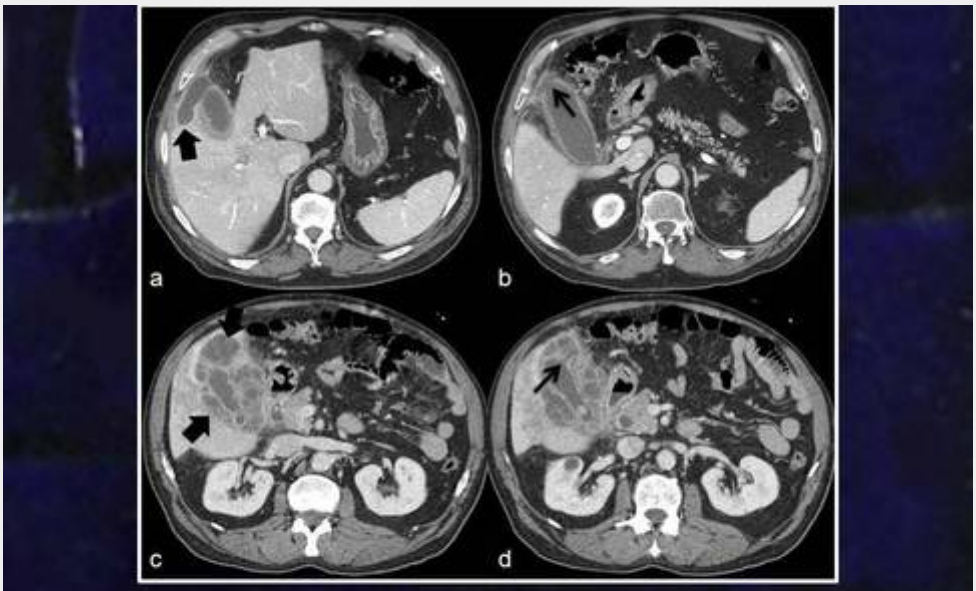

Fig. 3- Acute complicated cholecystitis

Two different cases of complicated cholecystitis (**a)** and **b)**; **c)** and **d)**) show perforation of the gallbladder wall (thin arrows on **b)** and **d)**) with formation of a pericholecystic abscess (thick arrows on **a)** and **c)**).

Several other conditions may cause acute pain in the RUQ (Figs. 4, 5, 6, 7, 8):

slide4.jpg

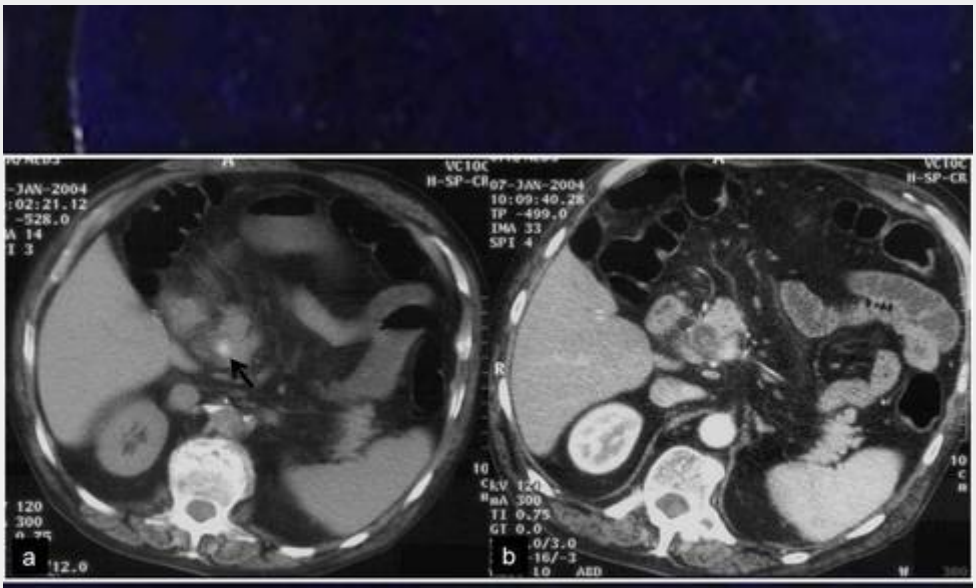

Fig. 4- Acute biliary colic

a) Non-enhanced CT clearly shows a spontaneous hyperdense stone located in the distal main biliary duct (black arrow); **b)** On contrast-enhanced CT the stone becomes much less visible, conveying the interest of obtaining plain scans in this setting; there is also dilatation of the main biliary duct with fluid.

slide5.jpg

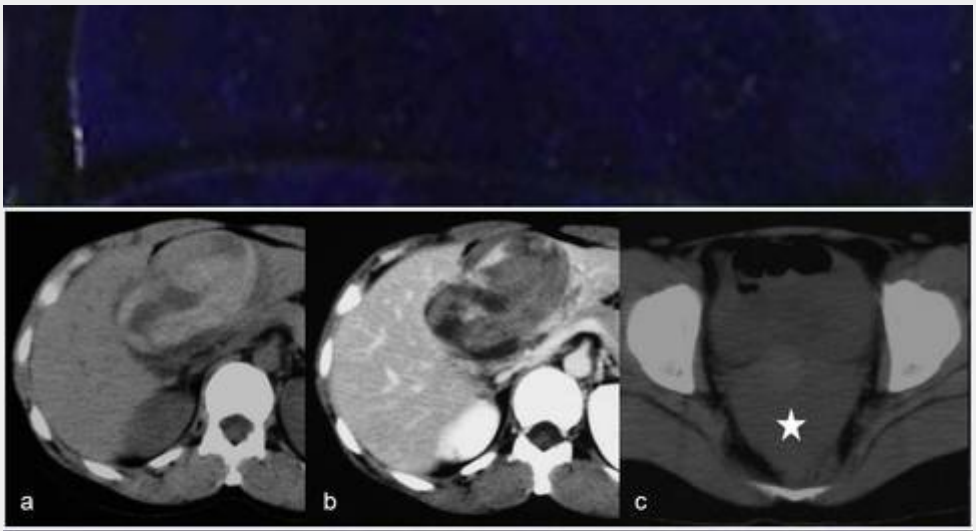

Fig. 5- Ruptured hepatic neoplasm

a) Non-enhanced CT demonstrates a spontaneous hyperdense liver mass corresponding to a haemorrhagic hepatocellular adenoma; **b)** On contrast-enhanced CT the focal liver lesion shows some heterogeneous enhancement but less than that of the adjacent parenchyma; **c)** Non-enhanced pelvic scan depicts a moderate amount of slightly hyperdense (haemorrhagic) fluid (white star).

slide6.jpg

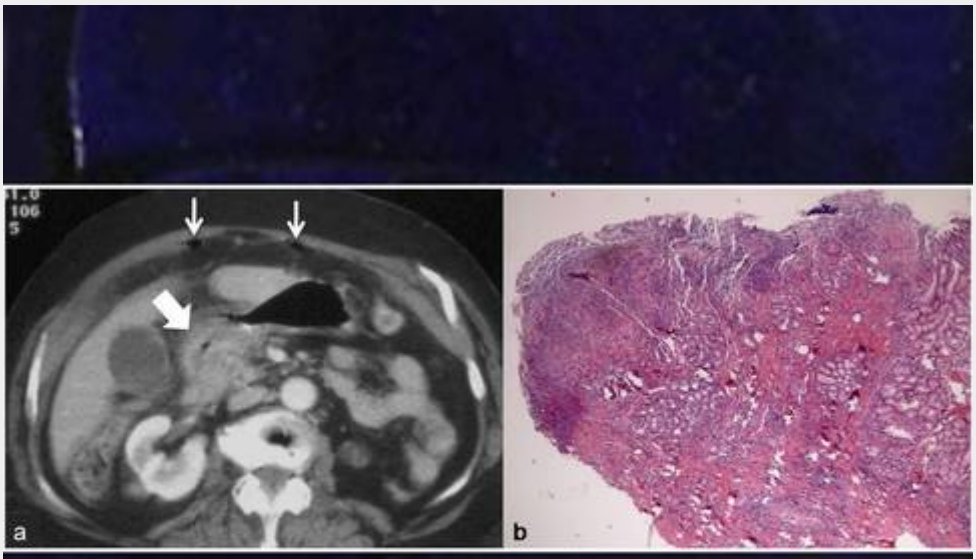

Fig. 6- Perforated peptic duodenal ulcer

a) Contrast-enhanced CT shows parietal thickening of the duodenal bulb (thick arrow) and small amounts of intra-peritoneal gas (thin arrows); **b)** Histology (H&E, 50x) shows inflammatory changes with granulation tissue and necrosis corresponding to the margins of the perforation.

slide7.jpg

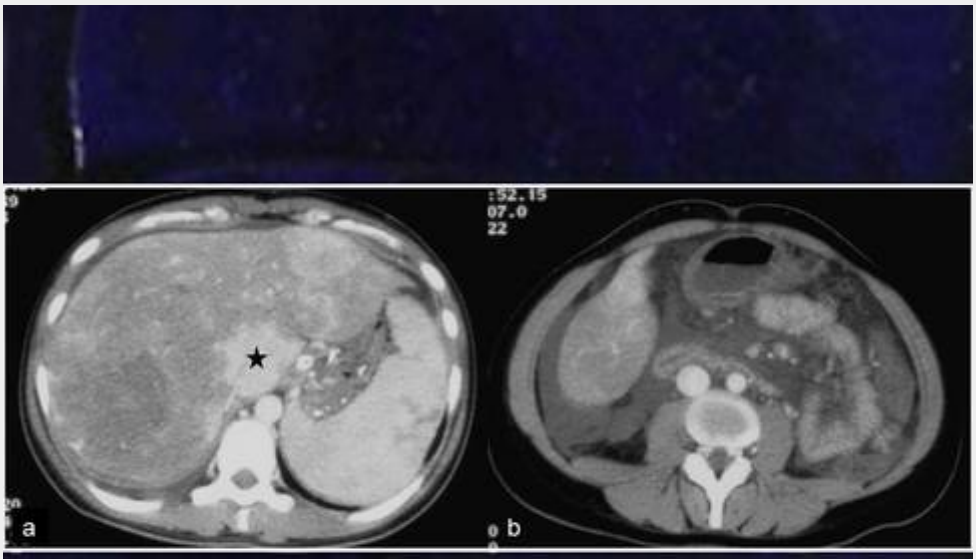

Fig. 7- Acute Budd-Chiari syndrome

a) Contrast-enhanced CT depicts a moderately enlarged liver with characteristic patchy enhancement and sparing of the caudate lobe (black star), and also a small amount of peritoneal fluid, which is much more evident on **b)**.

slide8.jpg

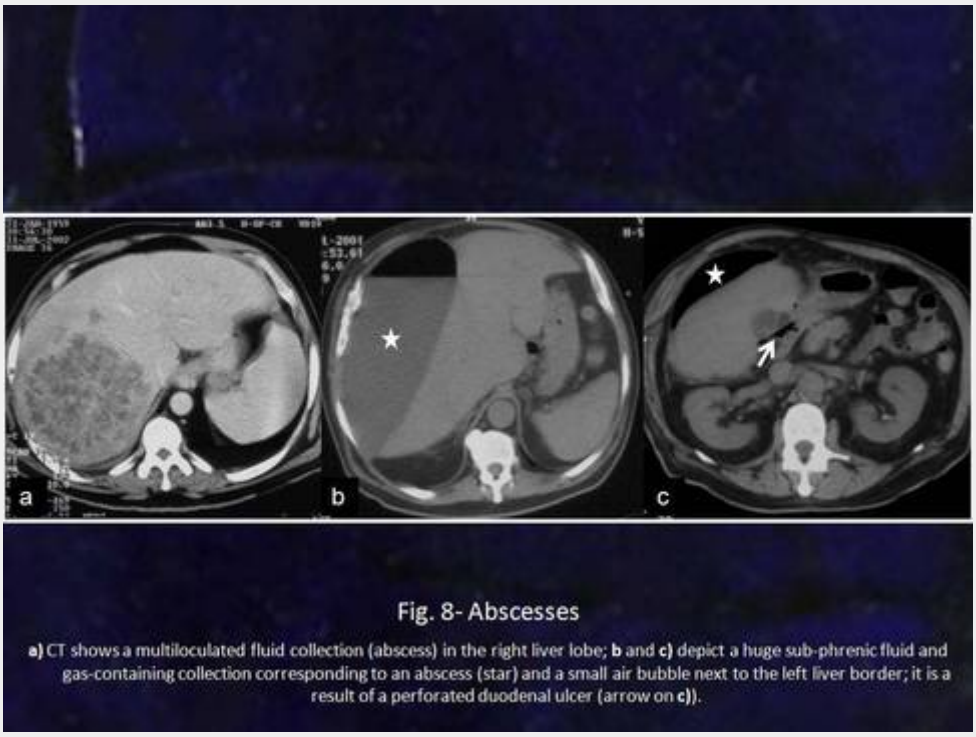

Fig. 8- Abscesses

a) CT shows a multiloculated fluid collection (abscess) in the right liver lobe; **b** and **c)** depict a huge sub-phrenic fluid and gas-containing collection corresponding to an abscess (star) and a small air bubble next to the left liver border; it is a result of a perforated duodenal ulcer (arrow on **c)**).

Acute pain in the LUQ is relatively infrequent and has a limited number of causes (Figs. 9, 10, 11).

slide9.jpg

slide10.jpg

Fig. 10- Splenic infarctions

Contrast-enhanced CT shows hypodense areas in the splenic parenchyma of a patient with a haematological disorder presenting with acute left upper quadrant pain.

slide11.jpg

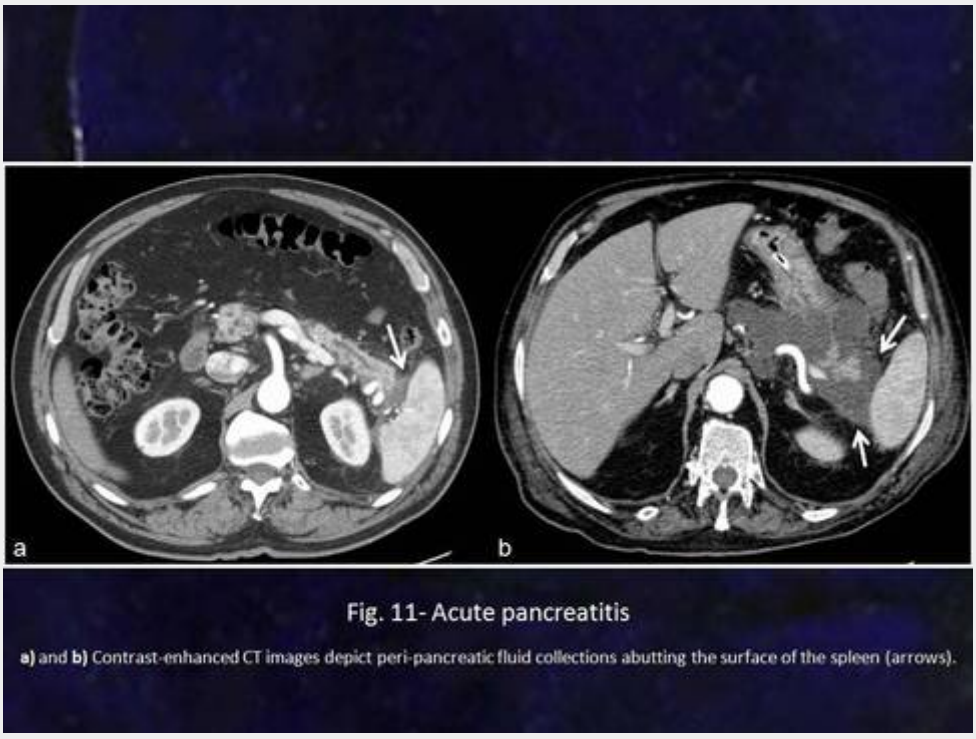

Fig. 11- Acute pancreatitis

a) and **b)** Contrast-enhanced CT images depict peri-pancreatic fluid collections abutting the surface of the spleen (arrows).

The most important cause of acute LLQ pain is acute diverticulitis (Fig.12).

slide12.jpg

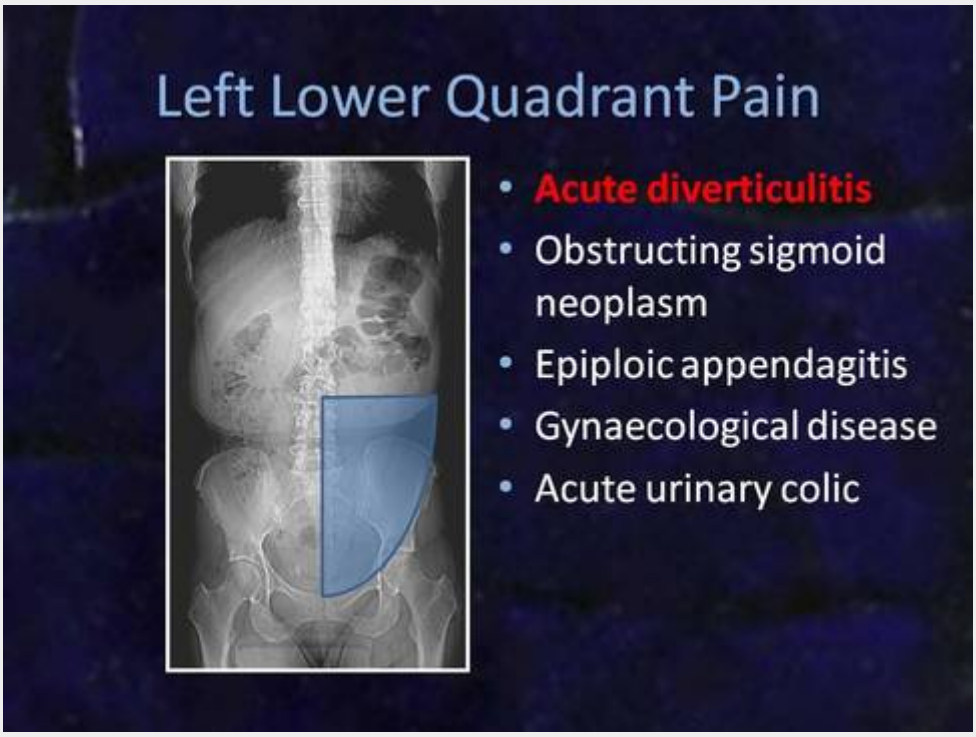

Acute diverticulitis may manifest as (Fig. 13):

- -Peri-colonic fat stranding (98% of cases)
- -Segmental colonic wall thickening > 4mm (70% of patients)
- -Peri-colonic fluid
- -Engorgement of mesenteric vessels
- -Complications (Fig. 14)
- - – Walled-off perforation
  - – Intra-peritoneal perforation
  - – Abscess (35%)
  - – Fistula (14%)
  - – Bowel obstruction (12%)

slide13.jpg

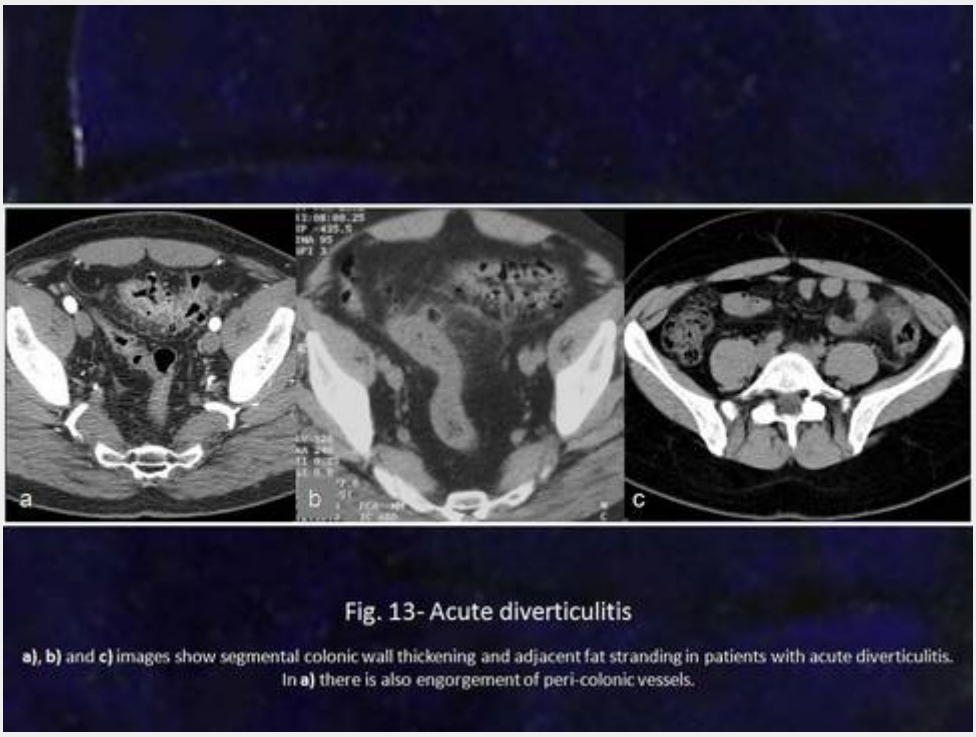

Fig. 13- Acute diverticulitis

a), b) and **c)** images show segmental colonic wall thickening and adjacent fat stranding in patients with acute diverticulitis. In **a)** there is also engorgement of peri-colonic vessels.

slide14.jpg

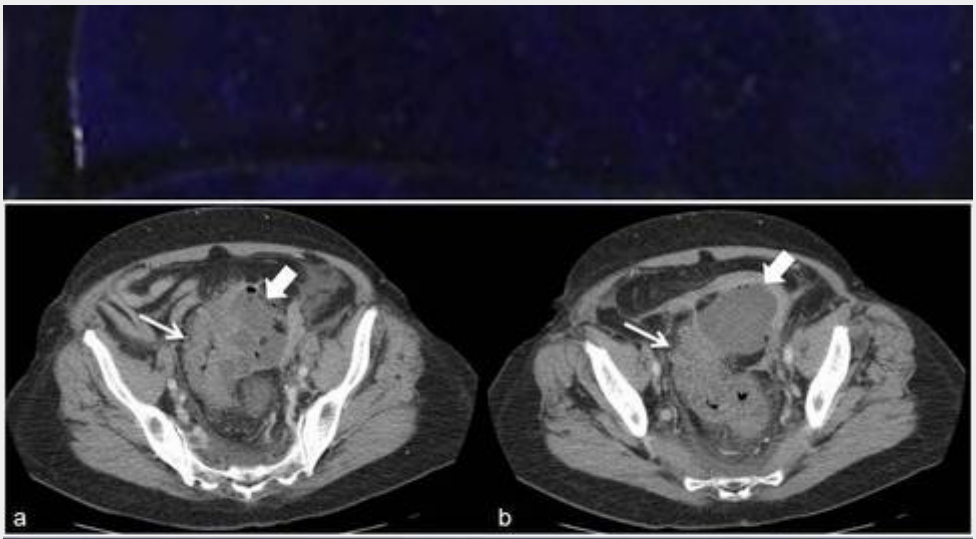

Fig. 14- Complicated acute diverticulitis

a) and **b)** Contrast-enhanced CT images depict thickening of the sigmoid wall (thin arrows) and adjacent fat stranding in a patient with acute diverticulitis complicated by a peri-colonic abscess containing small gas bubbles (thick arrows).

CT has high sensitivity, specificity and accuracy (respectively 93% and near 100%) in the diagnosis of acute diverticulitis, being also highly sensitive in the depiction of extra-colonic complications.

Various other mimickers may occur (Figs. 15, 16):

slide15.jpg

Fig. 15- Epiploic appendagitis

CT image reveals a lesion adjacent to the sigmoid colon (arrow) consisting of a fatty centre and a soft-tissue density rim at the periphery.

slide16.jpg

Fig. 16- Gynaecological disease

A cyst in the left adnexal region is shown by this CT image; it has a heterogeneous content with a fluid-fluid level, indicating the presence of internal haemorrhage.

The most frequent cause of acute RLQ pain is acute appendicitis (Fig.17).

slide17.jpg

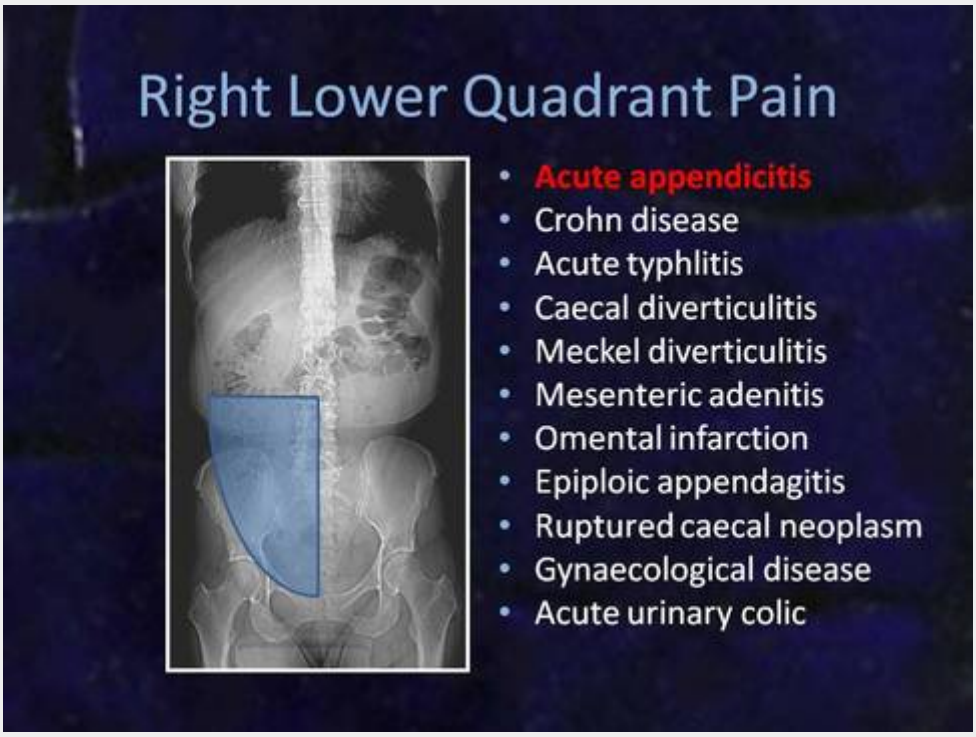

In acute appendicitis, CT may show (Fig. 18):

- -Fluid-filled enlarged appendix (highly specific)
- -Focal caecal apical thickening (highly specific)
- -Peri-appendiceal fat stranding (most sensitive sign)
- -Calcified appendicoliths
- -Appendiceal wall enhancement
- -Peri-appenciceal fluid
- -Perforation
- - – Phlegmon
  - – Abscess (Fig. 19)

slide18.jpg

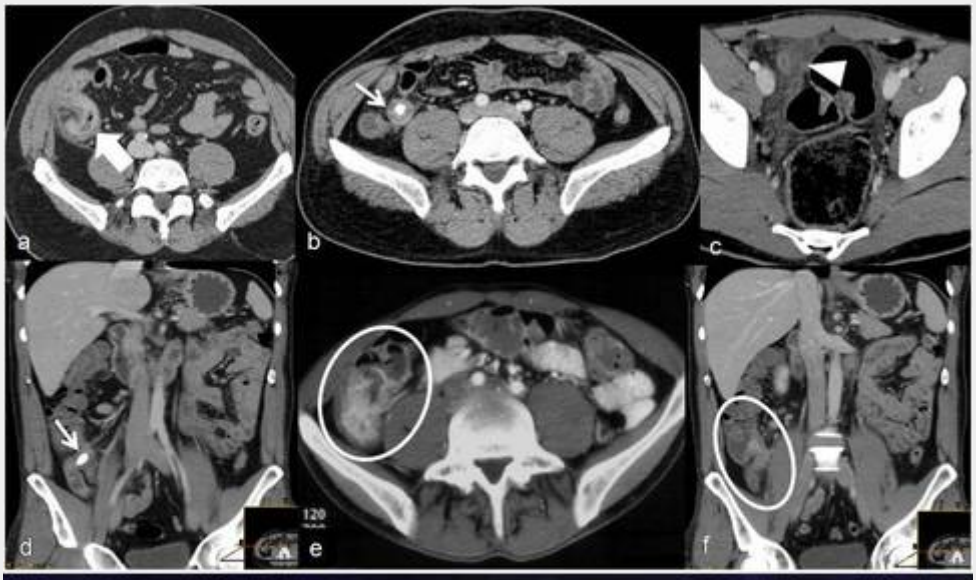

Fig. 18- Acute appendicitis

a) An enlarged, fluid-filled appendix with enhancement of the thickened wall and adjacent fat stranding (thick arrow) is shown; **b)** CT discloses a thick-walled appendix containing an appendicolith (thin arrow); **c)** there is a small quantity of fluid surrounding the inflamed appendix (arrowhead); **d)** a calcified appendicolith is seen within the appendiceal lumen (thin arrow); **e)** and **f)** images reveal focal caecal wall thickening (ellipses).

slide19.jpg

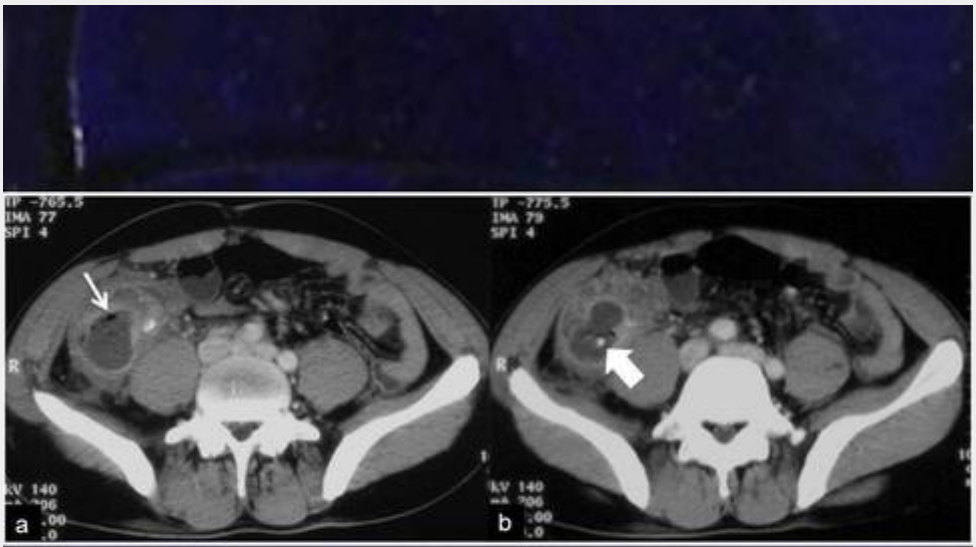

Fig. 19- Complicated acute appendicitis

a) and **b)** Contrast-enhanced CT images disclose a thick-walled fluid collection containing small gas bubbles (thin arrow on **a)**) and also calcified appendicoliths (thick arrow on **b)**), corresponding to an appendiceal abscess .

Acute appendicitis may be efficiently detected by CT studies, which have high sensitivity (90-100%), specificity (83-97%) and accuracy (93-98%) in the diagnosis of this condition. Non-visualization of the appendix on CT virtually excludes acute appendicitis. As a consequence, this method may contribute

to decrease the rate of negative laparotomies in patients with RLQ pain.

Other disorders may present with acute pain in the RLQ (Figs. 20, 21, 22, 23, 24):

slide20.jpg

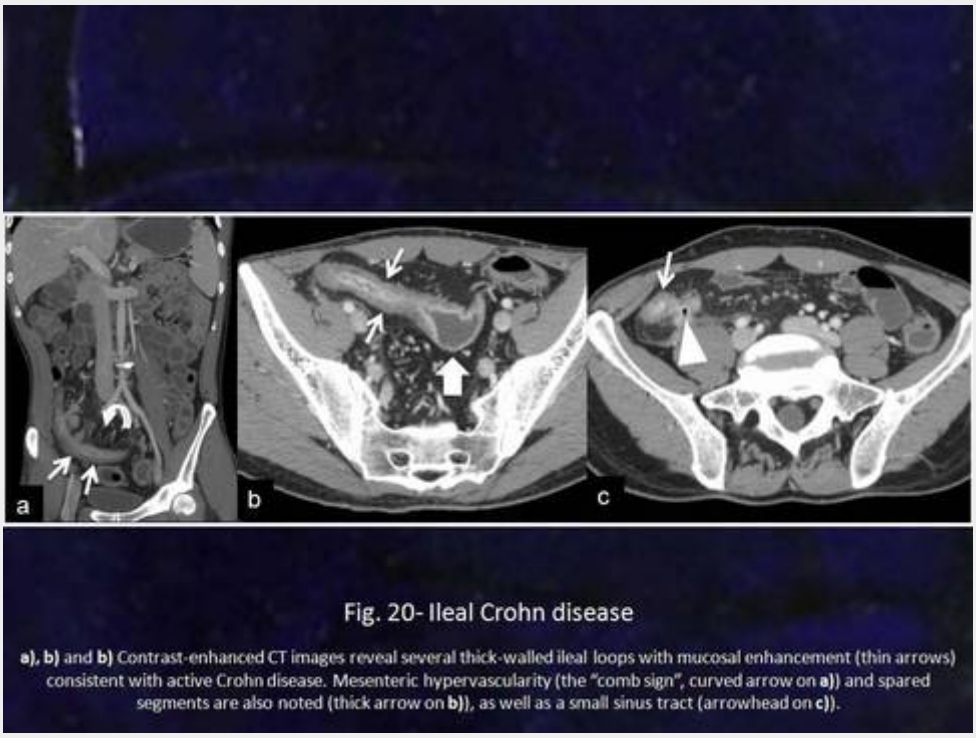

Fig. 20- Ileal Crohn disease

a), b) and **b)** Contrast-enhanced CT images reveal several thick-walled ileal loops with mucosal enhancement (thin arrows) consistent with active Crohn disease. Mesenteric hypervascularity (the "comb sign", curved arrow on **a)**) and spared segments are also noted (thick arrow on **b)**), as well as a small sinus tract (arrowhead on **c)**).

slide21.jpg

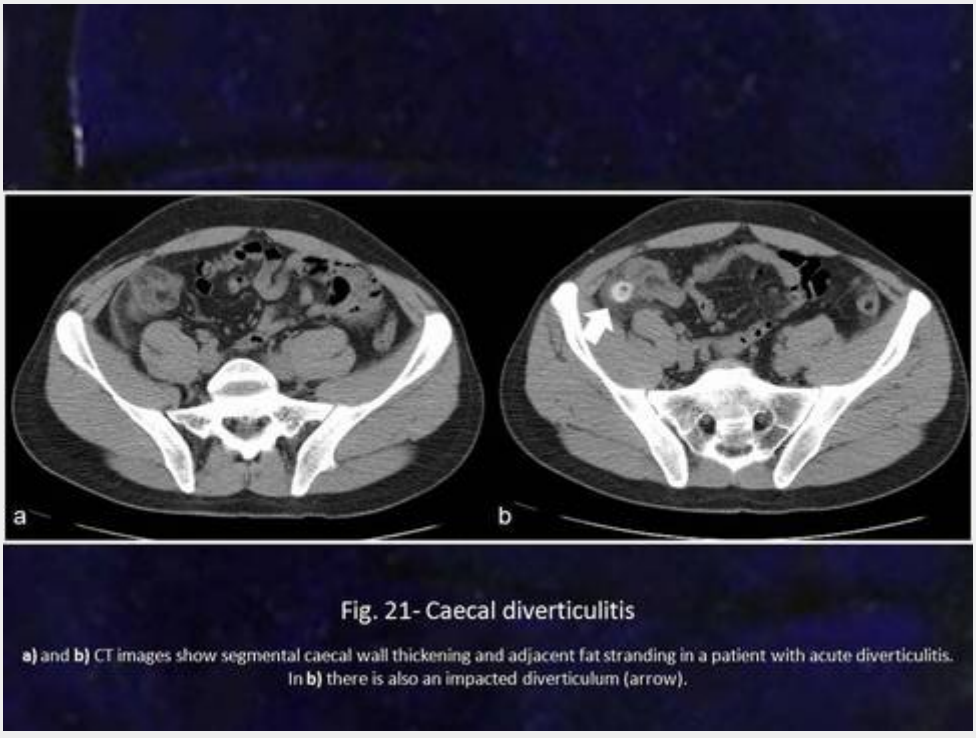

Fig. 21- Caecal diverticulitis

a) and **b)** CT images show segmental caecal wall thickening and adjacent fat stranding in a patient with acute diverticulitis. In **b)** there is also an impacted diverticulum (arrow).

slide22.jpg

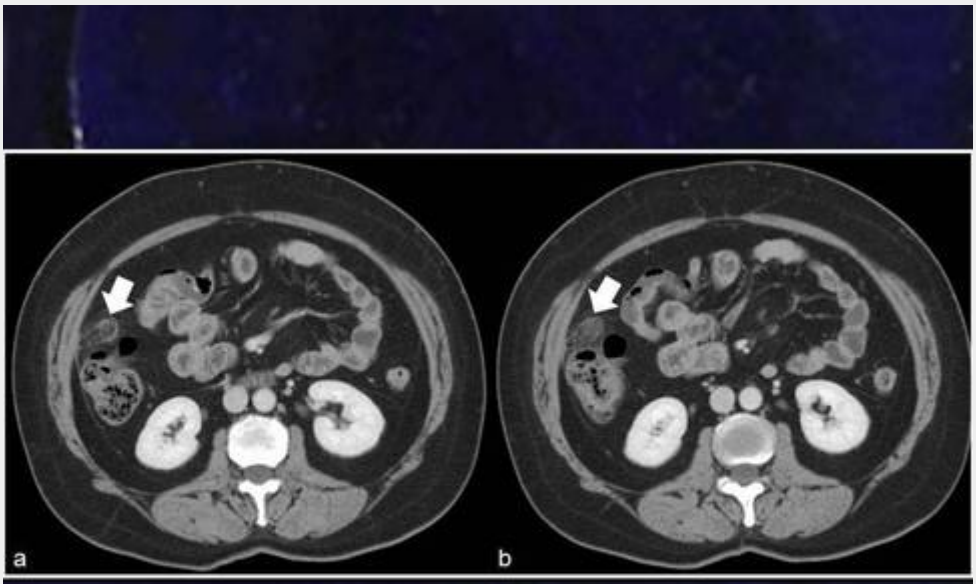

Fig. 22- Epiploic appendagitis

a) and **b)** images reveal a rounded mass adjacent to the ascending colon (arrows) displaying a central density of fat and a denser peripheral rim.

slide23.jpg

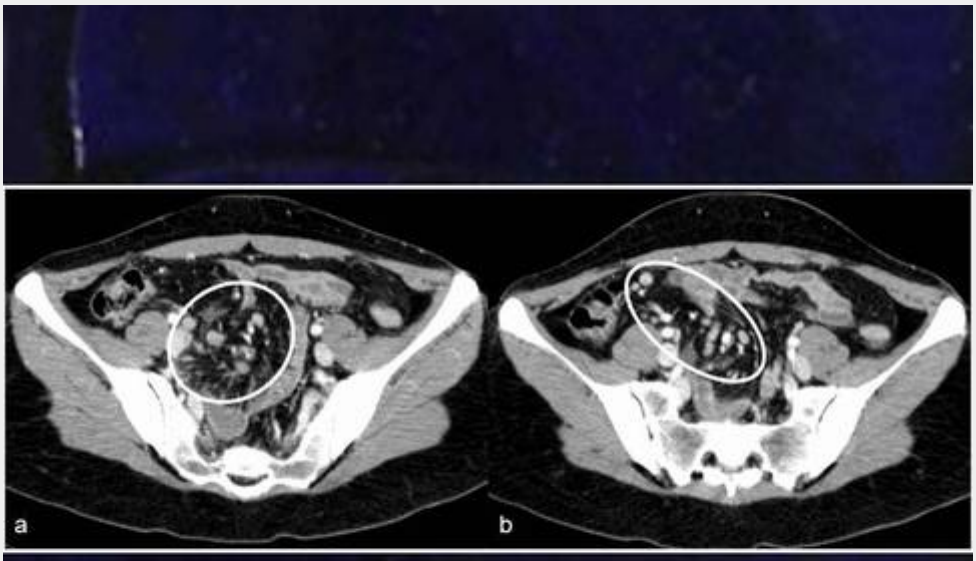

Fig. 23- Mesenteric adenitis

a) and **b)** images depict several enlarged mesenteric lymph nodes in a young patient with acute right lower quadrant pain, in the absence of other detectable abnormalities.

slide24.jpg

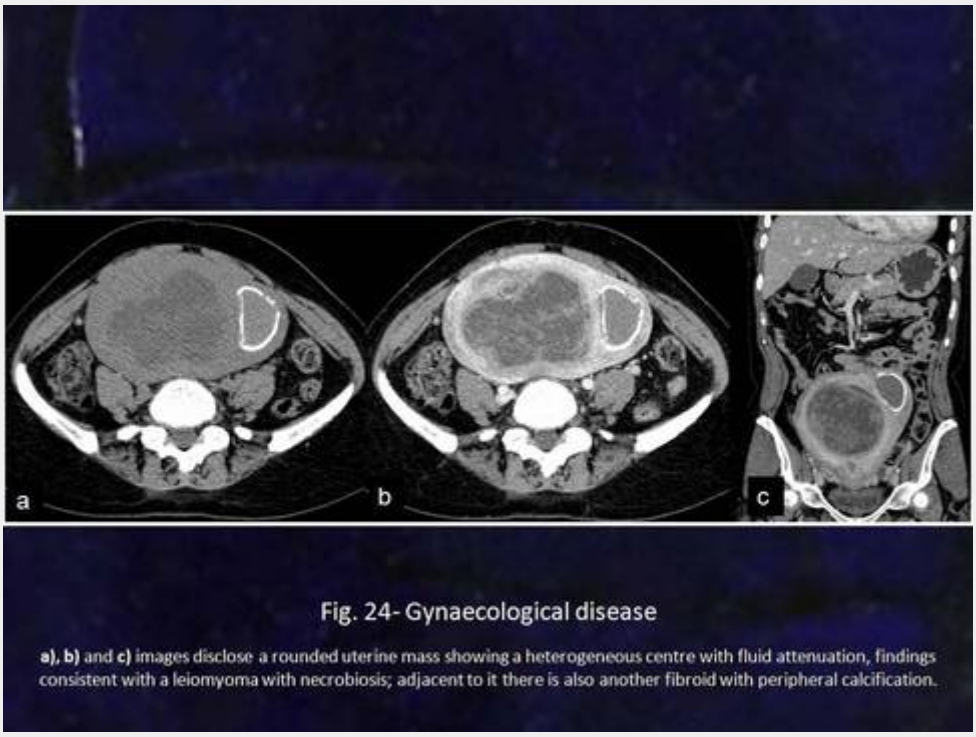

In cases of acute generalized pain, three main conditions may be implicated: bowel obstruction, ischemic bowel disease or gastrointestinal perforation (Fig. 25).

slide25.jpg

CT may be requested to differentiate a functional obstruction (paralytic ileus) from one with an underlying mechanical cause (mechanical ileus). Cases of paralytic ileus are generally related to post-operative states or secondary to ischemic conditions, inflammatory or infectious diseases, metabolic or hormonal abnormalities, drugs or innervation defects, and no organic lesion is found in these patients (Fig. 26).

slide26.jpg

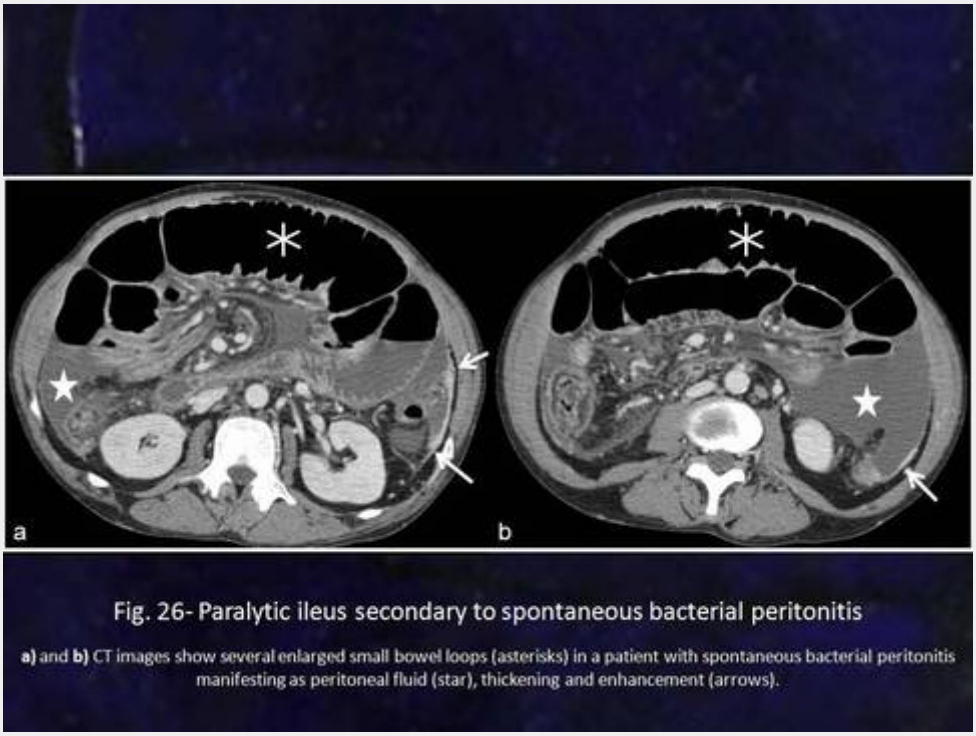

Fig. 26- Paralytic ileus secondary to spontaneous bacterial peritonitis

a) and **b)** CT images show several enlarged small bowel loops (asterisks) in a patient with spontaneous bacterial peritonitis manifesting as peritoneal fluid (star), thickening and enhancement (arrows).

The most frequent causes of SBO are related to adhesions and hernias, Crohn disease and, less commonly, neoplasms (Figs. 27, 28, 29); rarely, it may be due to other causes (Fig. 30). On the contrary, in LBO, carcinoma and diverticulitis are most often implicated, whereas volvulus remains an uncommon entity.

slide27.jpg

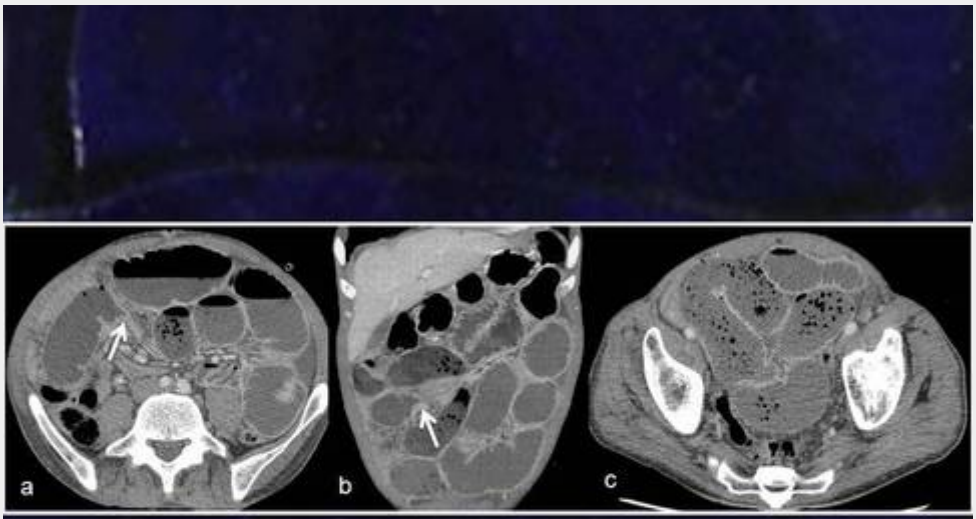

Fig. 27- Small bowel obstruction caused by an adhesion

Contrast-enhanced CT images depict signs of a SBO obstruction due to an adhesion, surgically confirmed. There is an abrupt transition zone (arrows on **a)** and **b)**) in the absence of a detectable organic lesion. The proximal bowel is distended with fluid and tiny air bubbles (**c**)), an appearance similar to faecal content ("small bowel faeces sign").

slide28.jpg

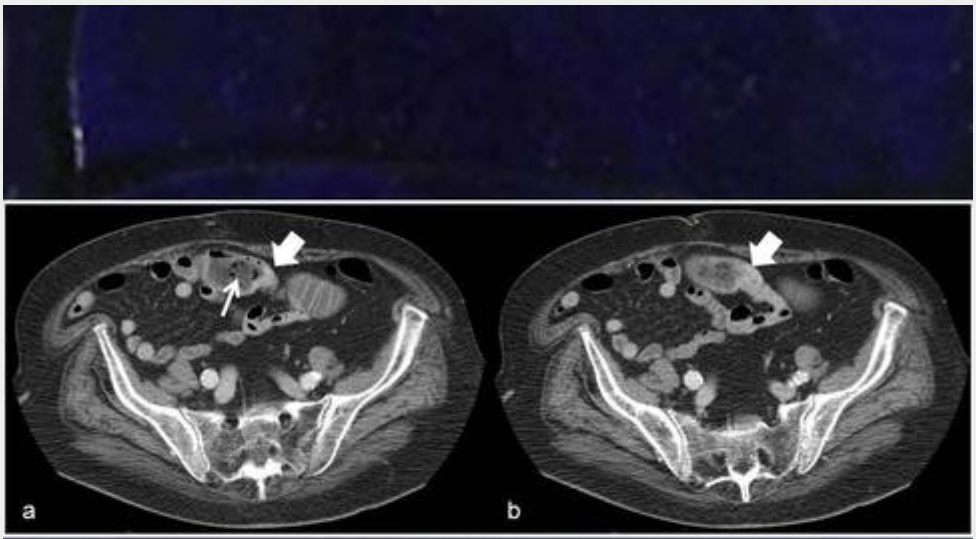

Fig. 28- Small bowel obstruction due to a jejunal adenocarcinoma

a) and **b)** An abrupt transition zone from the distended to the decompressed jejunum due to an adenocarcinoma manifesting also as a thickening of the bowel wall (thick arrows) is seen. The proximal bowel is distended with fluid mixed with tiny air bubbles (thin arrow on **a)**), resembling faecal content (the "small bowel faeces sign").

slide29.jpg

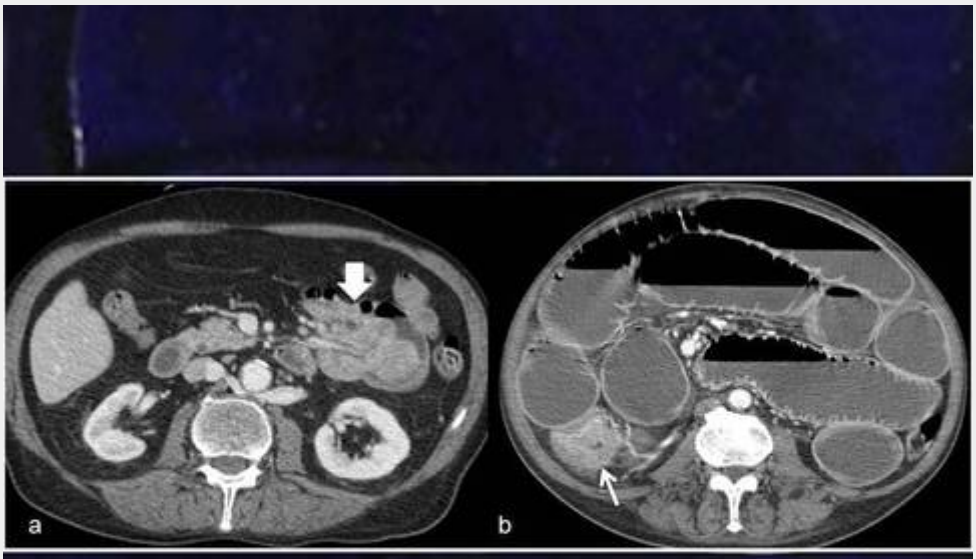

Fig. 29- Small bowel obstruction caused by neoplasm

a) In a patient with low-grade obstruction, CT depicts a small bowel neoplasm causing an intussusception (thick arrow); **b)** This high-grade obstruction is caused by a proximal colonic adenocarcinoma manifesting as bowel wall thickening (thin arrow). The proximal bowel is markedly distended with fluid and gas.

slide30.jpg

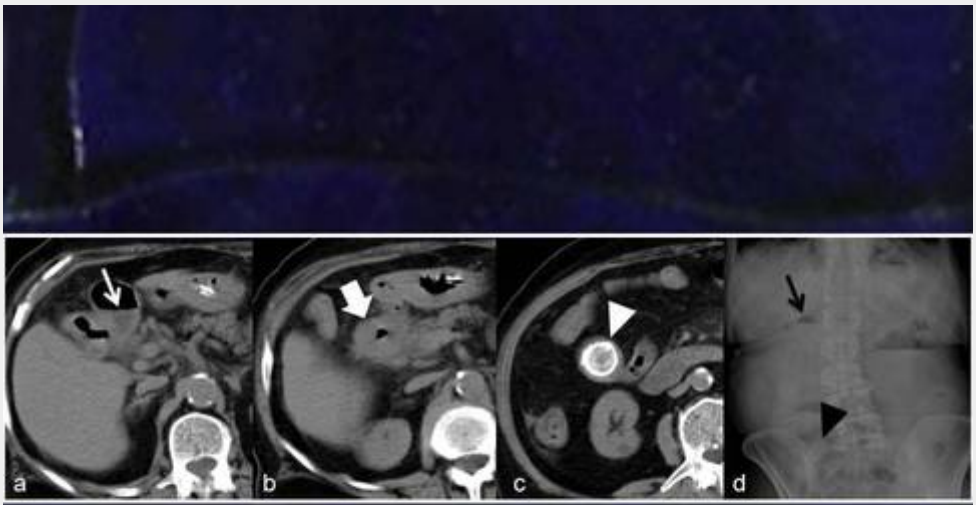

Fig. 30- Gallstone ileus

a) and **b)** CT images show an air-fluid level in the lumen of gallbladder (thin white arrow) and diffuse thickening of the duodenal wall (thick white arrow); **c)** A more caudal slice depicts a gallstone in the small bowel lumen (white arrowhead); **d)** Abdominal film also shows the air-fluid level in the gallbladder (thin black arrow) and the gallstone (black arrowhead).

The diagnosis of bowel obstruction relies on the identification of a transition zone from distended to decompressed bowel. In cases of malignant obstruction, this transition should be abrupt with irregular bowel wall thickening, sometimes accompanied by ancillary findings such as a mass or

lymphadenopathy. The diagnosis of adhesions, the most common cause of SBO, is one of exclusion in the majority of patients.

CT has the ability to easily identify the site, severity and cause of bowel obstruction and may depict complications (such as ischemia). This is especially true in cases of high-grade obstruction, where CT possesses high values of sensitivity (90-96%), specificity (91-96%) and overall accuracy (90-95%). However, CT performs considerably less well in patients with low-grade obstruction, in whom the accuracy of CT examinations may drop to approximately 50%.

In some patients, bowel obstruction may be a closed-loop process; in those cases, CT may demonstrate (Figs. 31, 32):

- -C- or U-shaped bowel loops
- -"Whirl sign" (twisting of mesenteric vessels)
- -Strangulation (Fig. 33)
- – Non-enhancement of a thickened bowel wall
- – Mesenteric oedema or haemorrhage
- – Engorgement of mesenteric vasculature
- – Ascites
- -Infarction
- – Gas in the bowel wall, mesenteric or portal veins

slide31.jpg

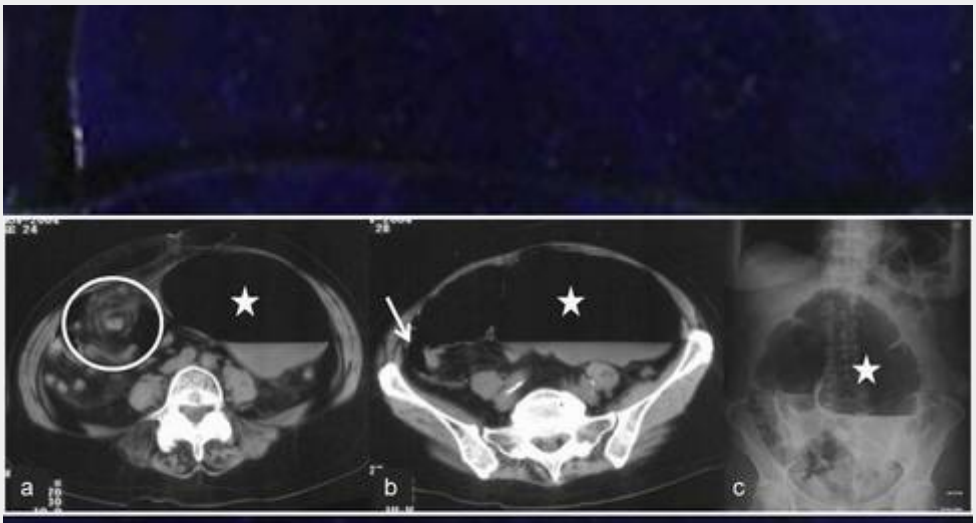

Fig. 31- Closed-loop LBO

a) and **b)** CT images depict a massively enlarged, gas and fluid-filled large bowel loop corresponding to a caecal volvulus (star); the diagnosis is also supported by a zone of twisting of the mesenteric vessels (white circle on **a)**) and a normally located ileo-caecal valve which however opens medially (arrow on **b)**); **c)** plain film shows an enlarged bowel loop with an air-fluid level, extending to the left abdominal quadrants.

slide32.jpg

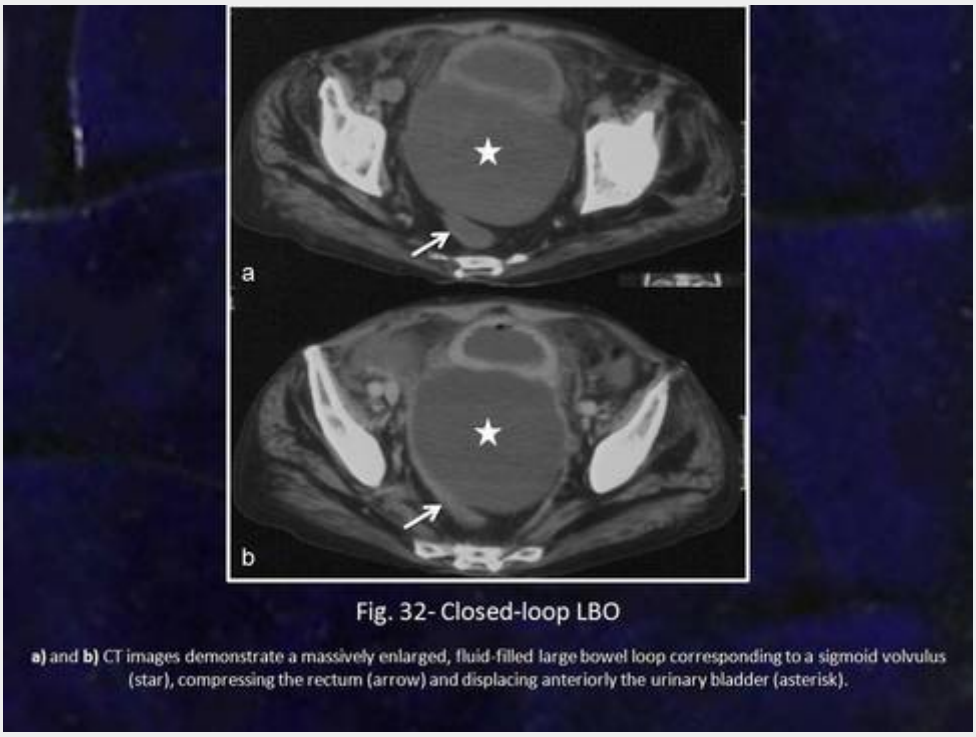

Fig. 32- Closed-loop LBO

a) and **b)** CT images demonstrate a massively enlarged, fluid-filled large bowel loop corresponding to a sigmoid volvulus (star), compressing the rectum (arrow) and displacing anteriorly the urinary bladder (asterisk).

slide33.jpg

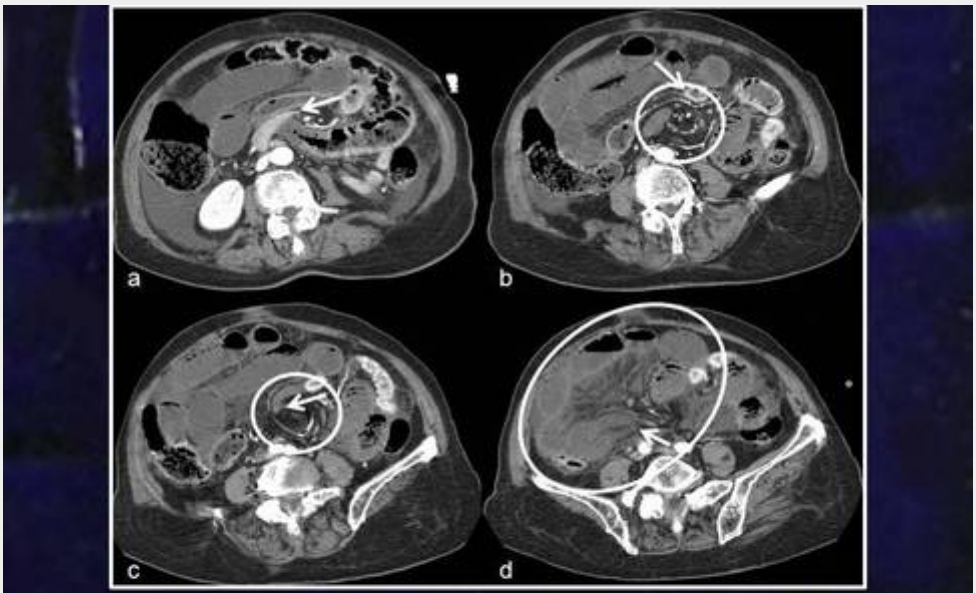

Fig. 33- Strangulated small bowel obstruction caused by an internal hernia

Contrast-enhanced CT images depict signs of a closed-loop obstruction due to a transmesenteric internal hernia, consisting of several beak-shaped SBO loops (arrows) and twisting of the mesenteric vessels (the "whirl sign", circles on **b)** and **c)**). There is also evidence of strangulation: non-enhancement of the thickened wall of several bowel loops to where engorged mesenteric vessels converge, mesenteric oedema/ haemorrhage, ascites (ellipse on **d)**).

Ischemic bowel disease may be a consequence of arterial occlusion, venous thrombosis or non-occlusive ischemia (hypoperfusion) (Fig. 34). Signs of ischemic bowel disease may include (Figs. 35, 36):

- -Filling defect in a mesenteric vessel
- -Bowel dilatation
- -Bowel wall thickening (oedema)
- -Diminished enhancement of the bowel wall
- -Mesenteric oedema and haemorrhage
- -Free intra-peritoneal fluid
- -Intestinal pneumatosis, portal and mesenteric venous gas (findings associated with a dismal prognosis)

slide34.jpg

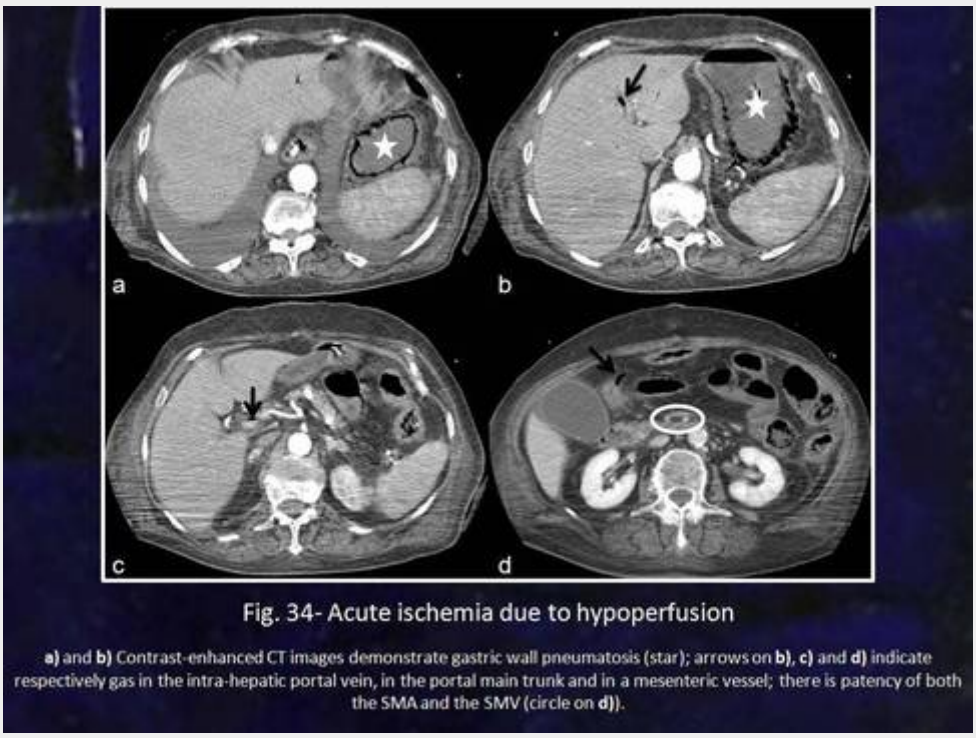

Fig. 34- Acute ischemia due to hypoperfusion

a) and **b)** Contrast-enhanced CT images demonstrate gastric wall pneumatosis (star); arrows on **b)**, **c)** and **d)** indicate respectively gas in the intra-hepatic portal vein, in the portal main trunk and in a mesenteric vessel; there is patency of both the SMA and the SMV (circle on **d)**).

slide35.jpg

Fig. 35- Ischemic bowel disease

a) and **b)** Contrast-enhanced CT images demonstrate filling defects in the spleno-mesenteric confluent (arrow on **a)**) and in the SMV with normal patency of the SMA (circle on **b)**); **c)** and **d)** show several dilated small bowel loops with thickened, poorly-enhancing wall, as well as mesenteric oedema/ haemorrhage and ascites.

slide36.jpg

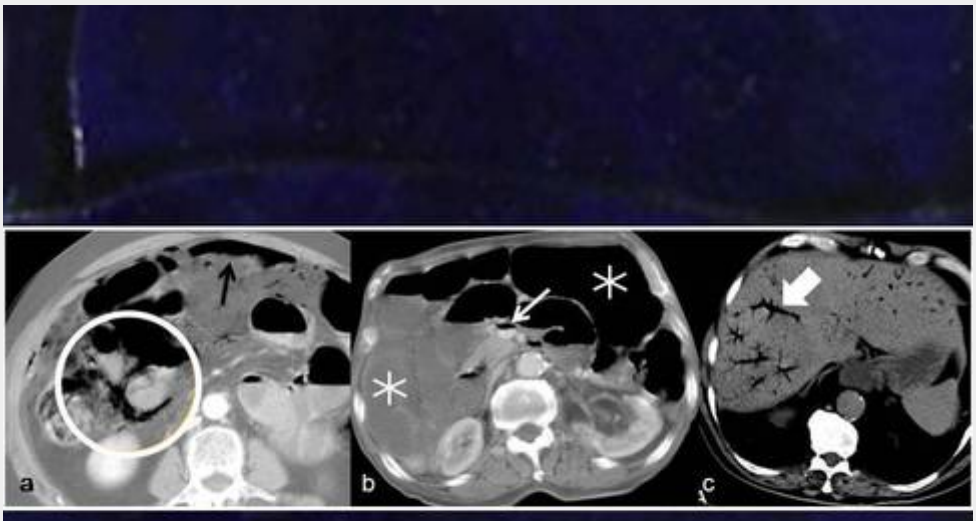

Fig. 36- Ischemic bowel disease

a) CT image demonstrate pneumatosis intestinalis (circle) and a small pneumoperitoneum (thin black arrow); thin white arrow on **b)** indicates gas in the SMV, as well as various dilated small bowel loops filled with gas and fluid (asterisks); **c)** CT image shows gas in the intra-hepatic portal vein branches (thick arrow). These findings are generally associated with a dismal prognosis.

GI tract perforation may be a result of peptic ulcer disease (Fig. 37), necrotic neoplasms (Fig. 38), ischemic or ulcerative colitis, diverticulitis and, increasingly, endoscopic instrumentation (Figs. 39, 40, 41).

CT signs of GI tract perforation include the following:

- -Pneumoperitoneum
- -Focal fluid
- -Extravasation of oral contrast
- -Local inflammatory changes in the bowel wall, adjacent fat and mesentery

slide37.jpg

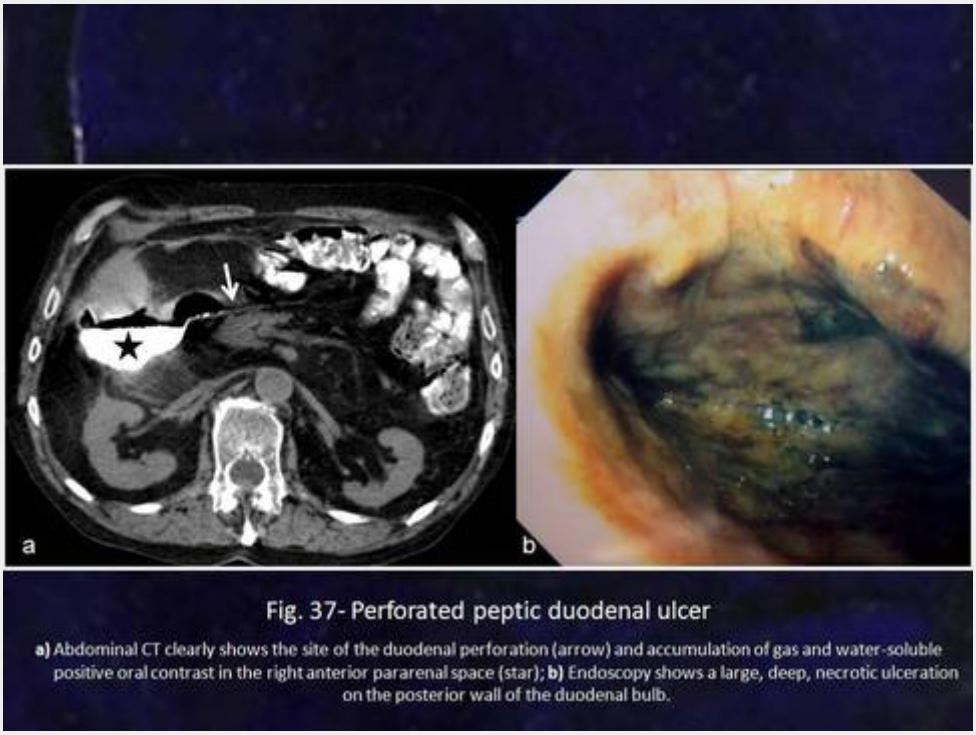

Fig. 37- Perforated peptic duodenal ulcer

a) Abdominal CT clearly shows the site of the duodenal perforation (arrow) and accumulation of gas and water-soluble positive oral contrast in the right anterior pararenal space (star); **b)** Endoscopy shows a large, deep, necrotic ulceration on the posterior wall of the duodenal bulb.

slide38.jpg

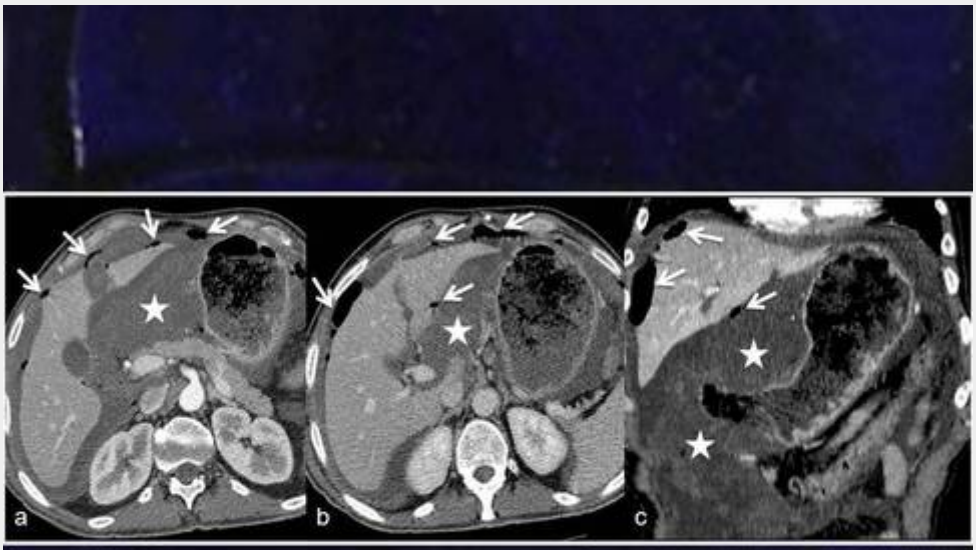

Fig. 38- Perforated gastric neoplasm

a), b) and **c)** images all demonstrate a huge heterogeneous gastric tumor (stars) which has ruptured and originated multiple pockets of intra-peritoneal gas (arrows). Note also the presence of abundant ascites.

slide39.jpg

Fig. 39- Duodenal perforation following ERCP with sphincterothomy for biliary lythiasis

a) and **b)** contrast-enhanced CT images performed with water-soluble positive oral contrast agent show retroperitoneal extravasation into the right anterior pararenal space (arrow) and abundant retroperitoneal gas. Note cholelythiasis, intra- and extra-hepatic aerobilia, and main pancreatic duct dilatation with severe atrophy of pancreatic parenchyma; **c)** and **d)** plain films reveal the extent of gas collections, with pneumoretroperitoneum and mediastinal, cervical, and subcutaneous emphysema.

slide40.jpg

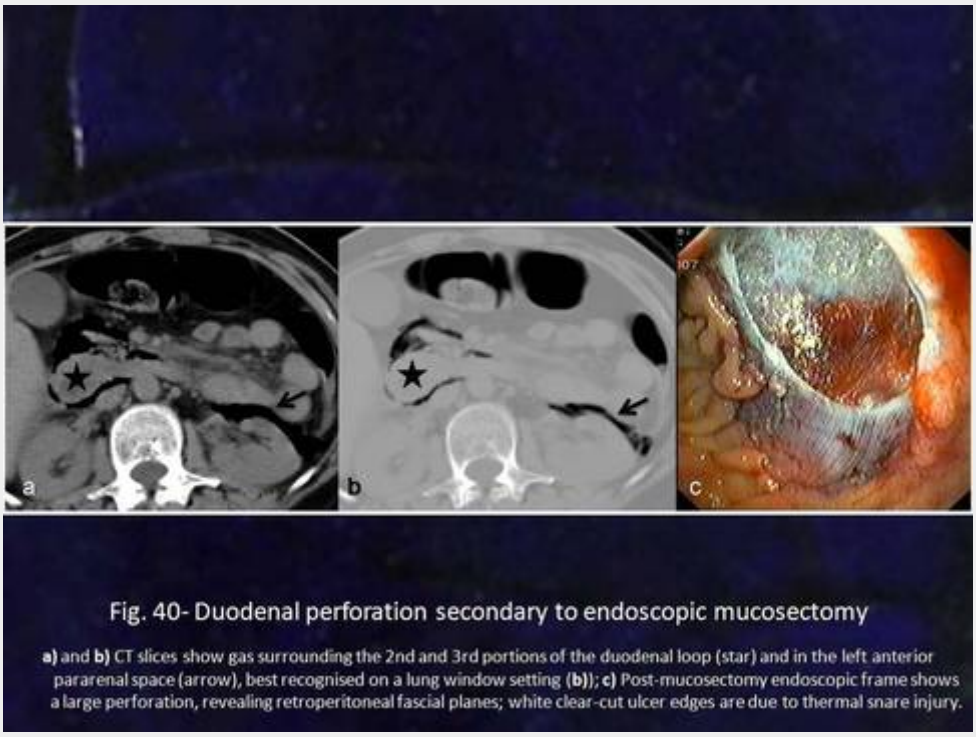

Fig. 40- Duodenal perforation secondary to endoscopic mucosectomy

a) and **b)** CT slices show gas surrounding the 2nd and 3rd portions of the duodenal loop (star) and in the left anterior pararenal space (arrow), best recognised on a lung window setting **(b))**; **c)** Post-mucosectomy endoscopic frame shows a large perforation, revealing retroperitoneal fascial planes; white clear-cut ulcer edges are due to thermal snare injury.

slide41.jpg

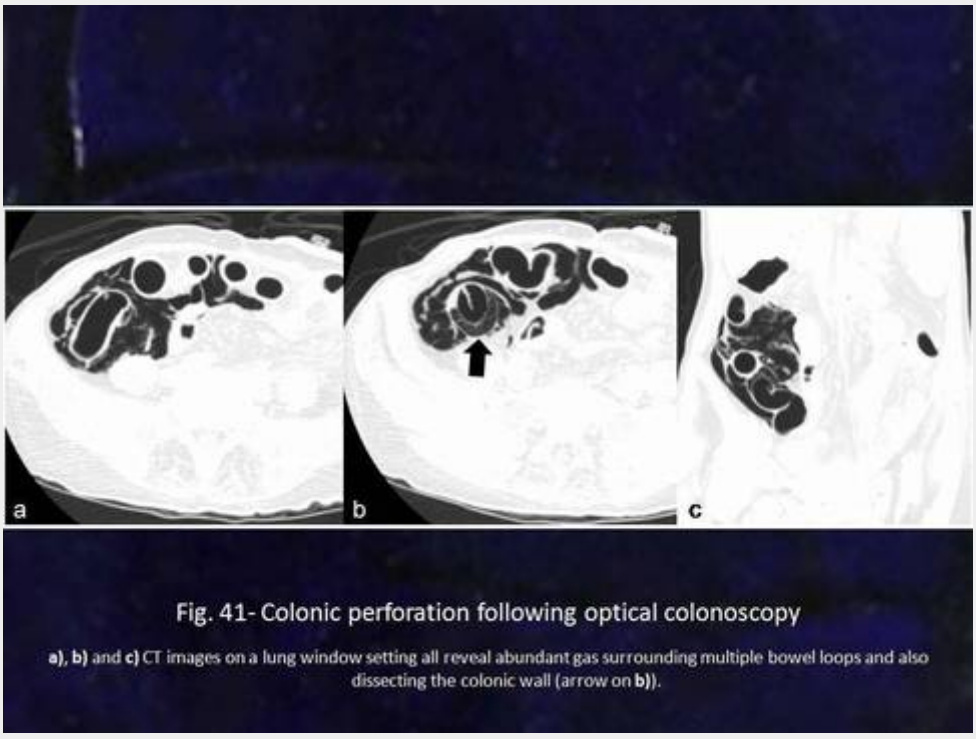

Fig. 41- Colonic perforation following optical colonoscopy

a), b) and **c)** CT images on a lung window setting all reveal abundant gas surrounding multiple bowel loops and also dissecting the colonic wall (arrow on **b)**).

CT can detect a pneumoperitoneum which is overlooked on conventional radiography; nevertheless, the precise site of perforation may be difficult to determine because the location of free air does not necessarily correlate with the local of perforation.

Additional conditions causing generalized acute pain are relatively rare (Fig. 42):

slide42.jpg

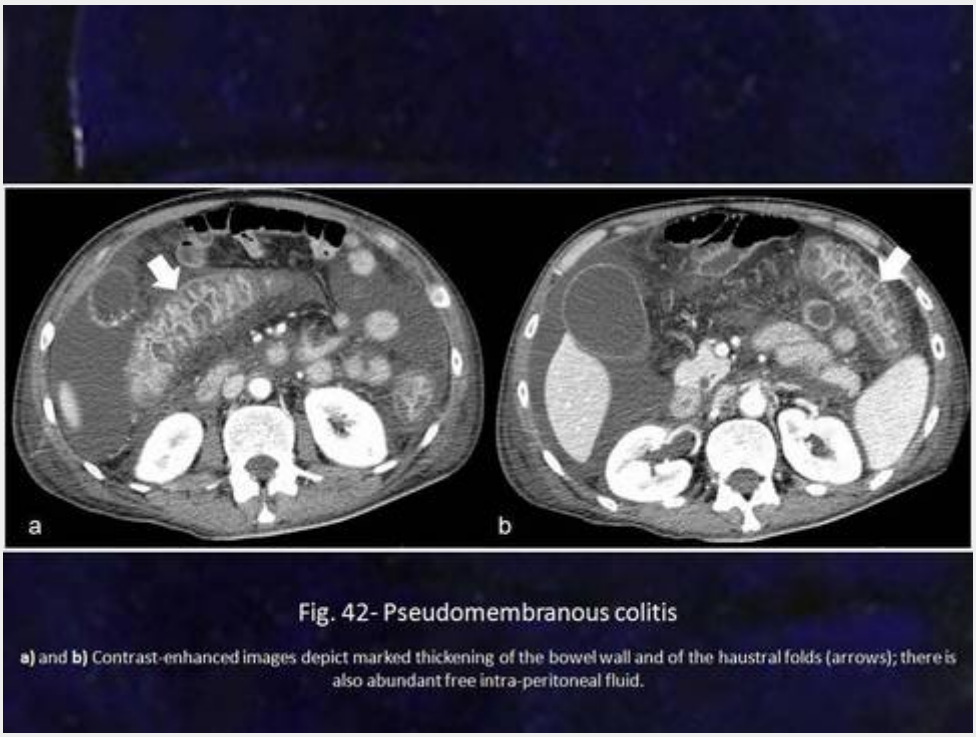

Fig. 42- Pseudomembranous colitis

a) and **b)** Contrast-enhanced images depict marked thickening of the bowel wall and of the haustral folds (arrows); there is also abundant free intra-peritoneal fluid.

Epigastric pain often results from acute pancreatitis (Fig. 43).

slide43.jpg

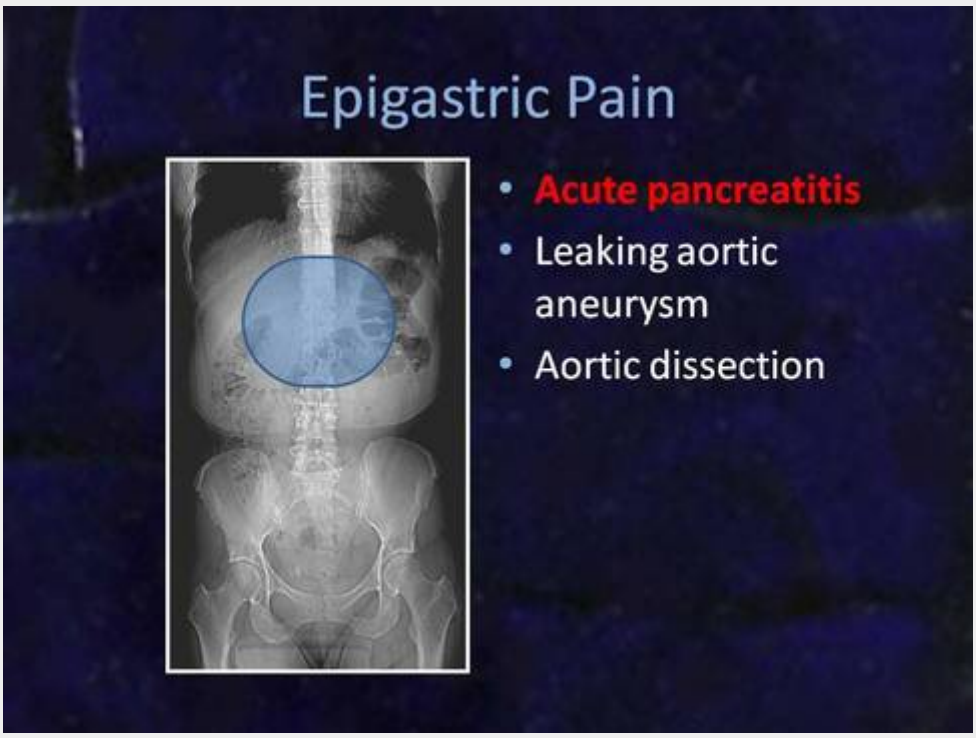

Although in mild forms CT scans may be normal (up to 28%of patients), imaging findings in acute pancreatitis are (Fig.44):

- -Gland enlargement
- -Parenchymal necrotic areas (absent enhancement)
- -Peri-pancreatic exudates and fluid collections
- - – Lesser sac
  - – Anterior para-renal space
  - – Mesenteric root
  - – Transverse mesocolon
- -Complications (Fig. 45)
- - – Pseudoaneurysms
  - – Thrombosis
  - – Abscesses

slide44.jpg

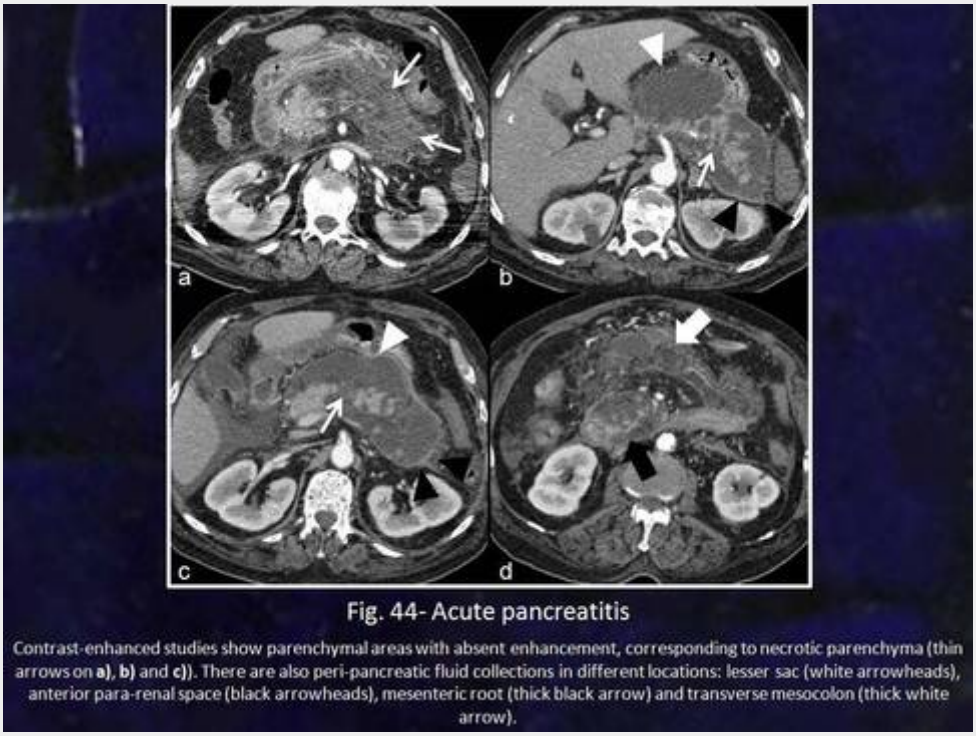

Fig. 44- Acute pancreatitis

Contrast-enhanced studies show parenchymal areas with absent enhancement, corresponding to necrotic parenchyma (thin arrows on **a)**, **b)** and **c)**). There are also peri-pancreatic fluid collections in different locations: lesser sac (white arrowheads), anterior para-renal space (black arrowheads), mesenteric root (thick black arrow) and transverse mesocolon (thick white arrow).

slide45.jpg

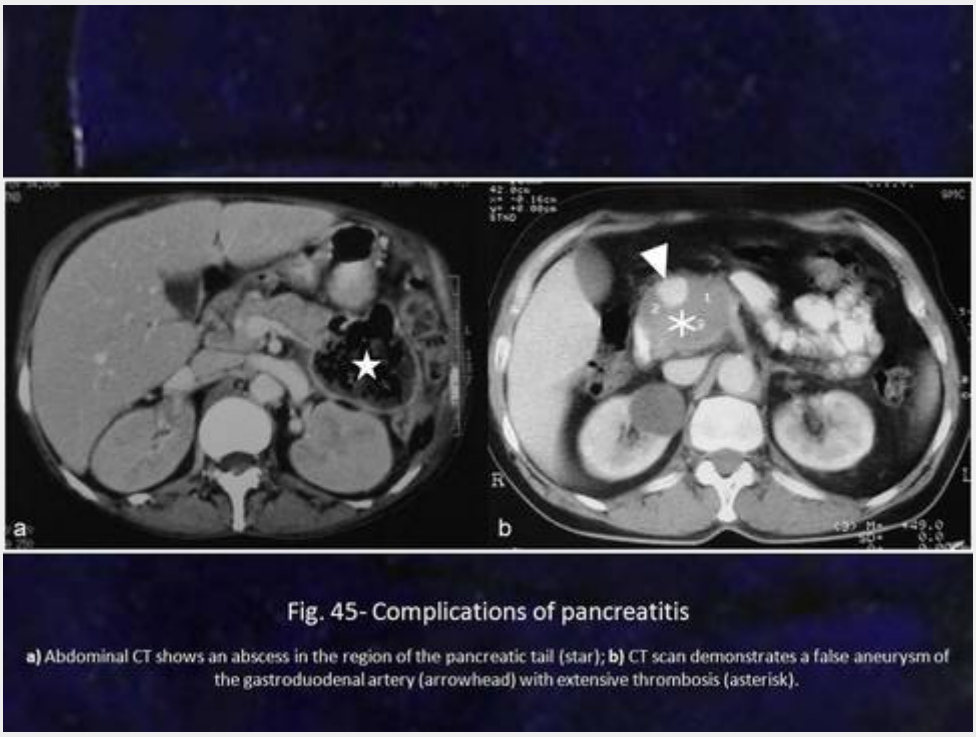

Fig. 45- Complications of pancreatitis

a) Abdominal CT shows an abscess in the region of the pancreatic tail (star); **b)** CT scan demonstrates a false aneurysm of the gastroduodenal artery (arrowhead) with extensive thrombosis (asterisk).

Several studies have determined that CT findings correlate well with the clinical severity of acute pancreatitis. Moreover, the degree of parenchymal necrosis predicts patient outcome. As a result, CT is the modality of choice for staging the extent of disease and for detecting complications.

Clinical mimickers are mainly attributable to acute aortic conditions (Fig. 46):

slide46.jpg

Flank pain has multiple causes, but urinary colic is the most frequent (Fig. 47).

slide47.jpg

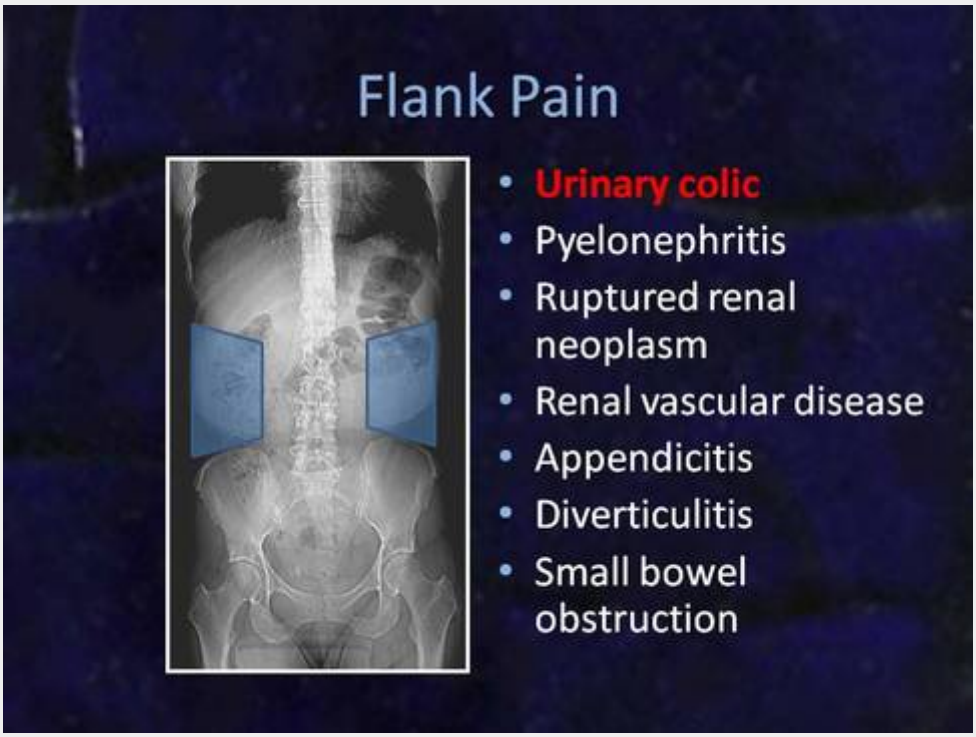

CT findings in acute urinary colic include (Fig. 48):

- -Radiopaque stone at ureteropelvic or ureterovesical junction
- -Peri-ureteral fat stranding
- -Hydronephrosis
- -Peri-nephric stranding
- -Renal enlargement

slide48.jpg

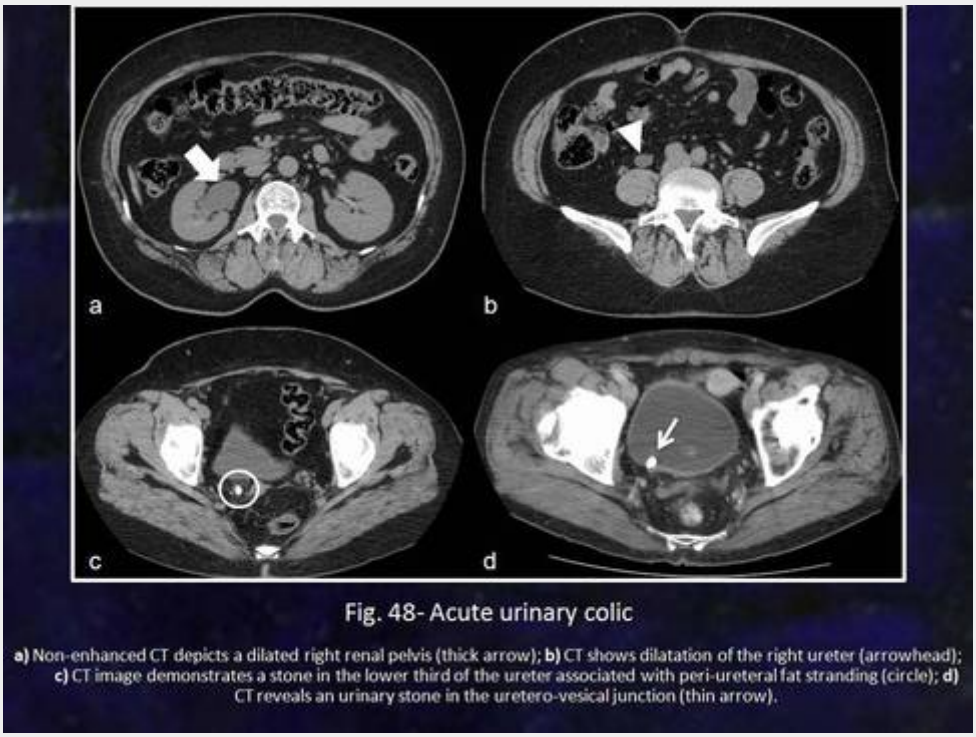

Fig. 48- Acute urinary colic

a) Non-enhanced CT depicts a dilated right renal pelvis (thick arrow); **b)** CT shows dilatation of the right ureter (arrowhead); **c)** CT image demonstrates a stone in the lower third of the ureter associated with peri-ureteral fat stranding (circle); **d)** CT reveals an urinary stone in the uretero-vesical junction (thin arrow).

CT is more accurate than conventional radiography or US for depicting urinary stones (sensitivity: 97%; specificity: 96%; accuracy: 97%) but care should be taken to obtain non-enhanced scans, since iv contrast may obscure radiopaque stones.

Various other disorders may be responsible for an acute flank pain (Figs. 49, 50, 51, 52, 53):

slide49.jpg

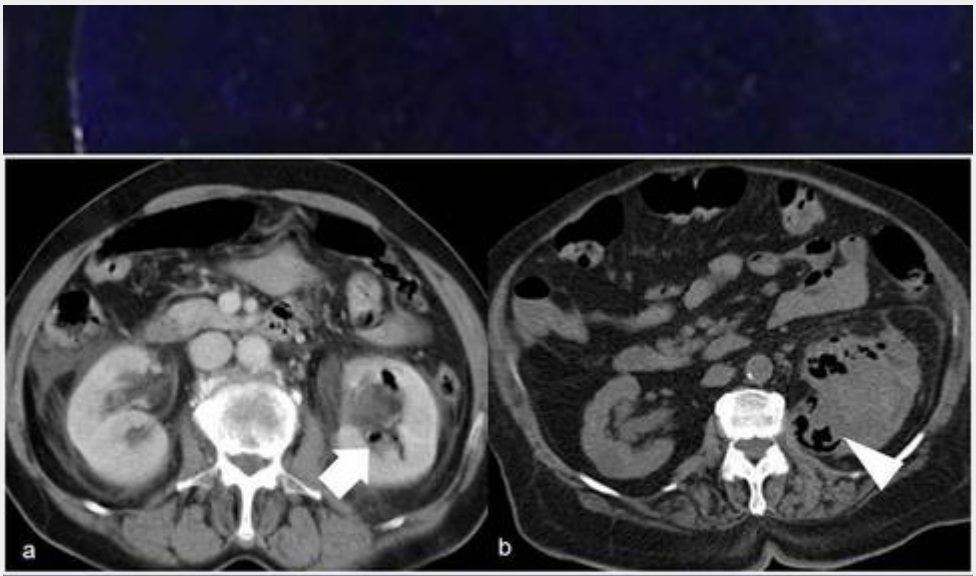

Fig. 49- Acute renal infection

a) Abdominal contrast-enhanced CT shows gas in the collecting system of the left kidney, corresponding to an emphysematous pyelitis (arrow); **b)** CT scan demonstrates parenchymal gas, characteristic of an emphysematous pyelonephritis (arrowhead).

slide50.jpg

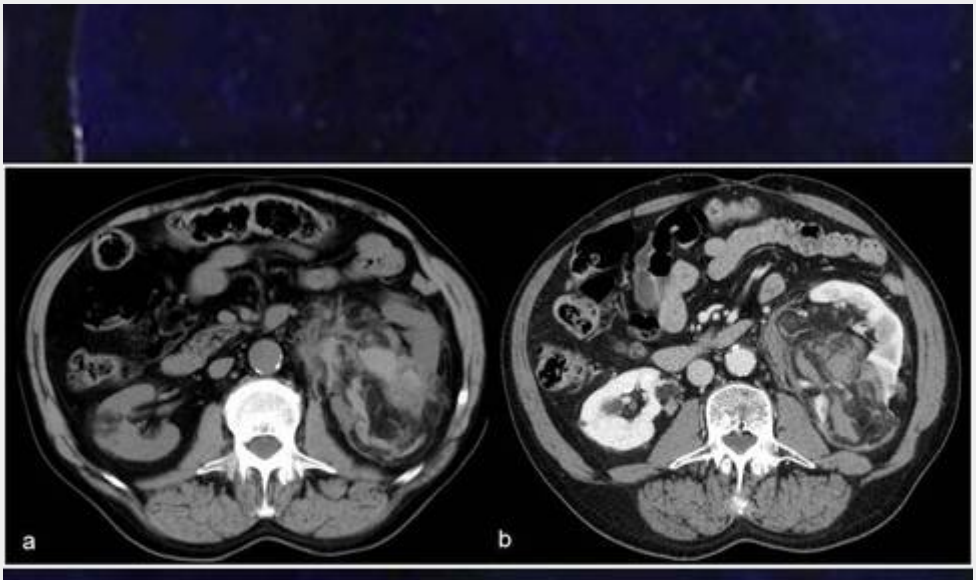

Fig. 50- Ruptured renal neoplasm

a) and **b)** CT slices demonstrate a predominantly fatty left renal mass with spontaneous hyperdense areas corresponding to a haemorrhagic angiomyolipoma. Note the presence of other angiomyolipomas in the opposite kidney.

slide51.jpg

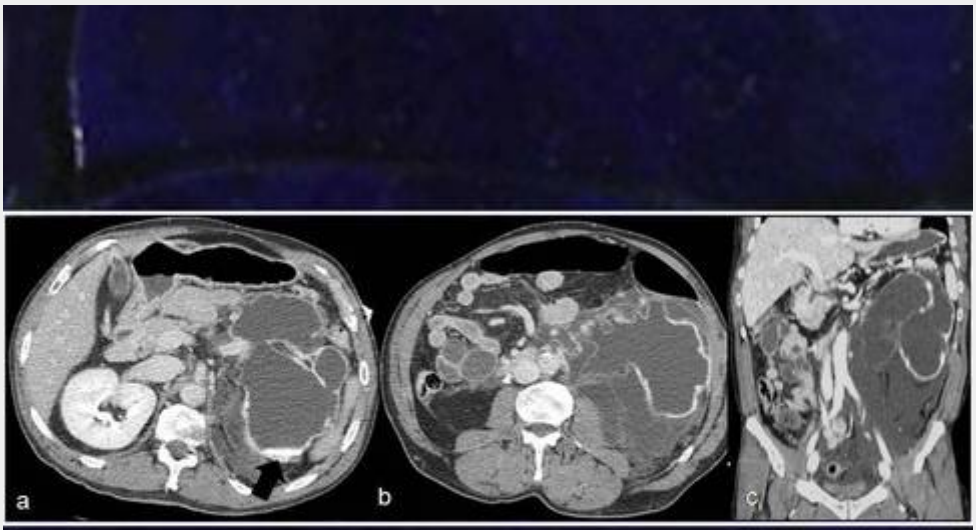

Fig. 51- Ruptured hydronephrotic kidney

a), b) and **c)** images demonstrate signs of rupture of a markedly hydronephrotic left kidney, represented by extensive retroperitoneal fluid outside the collecting system; there is contrast layering inside the dilated collecting system indicated by an arrow in **a)**.

slide52.jpg

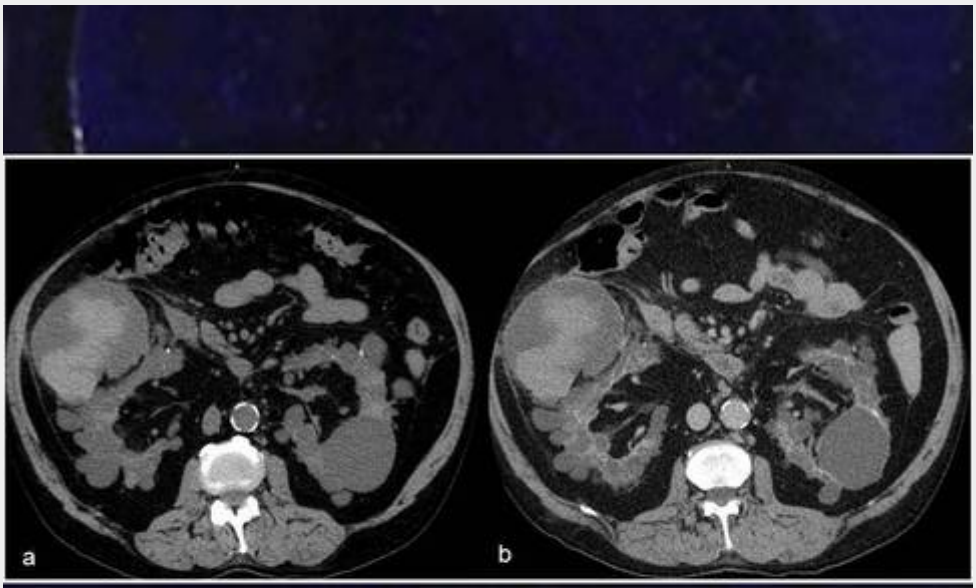

Fig. 52- Complicated renal cyst

a) and **b)** CT images show a right renal cyst with spontaneous hyperdense areas corresponding to haemorrhage in a patient with renal polycystic disease. Note also other non-complicated cysts distributed throughout both kidneys.

slide53.jpg

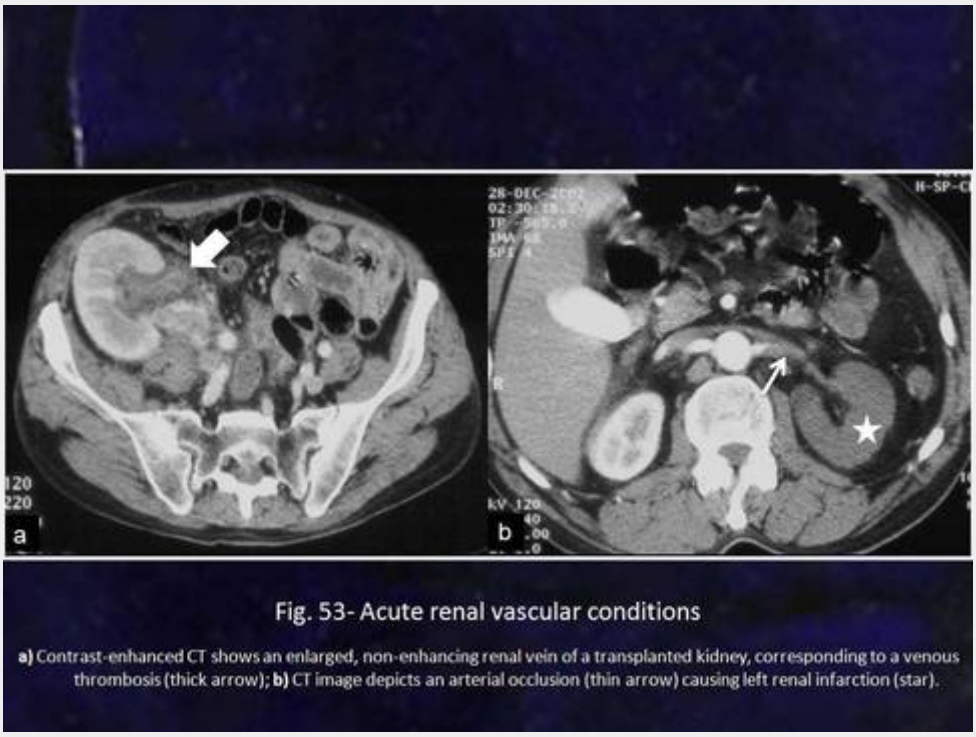

Fig. 53- Acute renal vascular conditions

a) Contrast-enhanced CT shows an enlarged, non-enhancing renal vein of a transplanted kidney, corresponding to a venous thrombosis (thick arrow); **b)** CT image depicts an arterial occlusion (thin arrow) causing left renal infarction (star).

4. Conclusion

CT is being increasingly seen as the first-line imaging method in the study of patients presenting with acute abdominal pain, since it lacks the disadvantages of plain films and ultrasonography and is able to replace them in a wide spectrum of situations. It is also a cost-effective, highly accurate (>95%) imaging modality in the majority of acute abdominal conditions. This method may additionally suggest alternative diagnoses different from the one initially suspected in a proportion of cases. The topographic classification of pain by abdominal quadrants may facilitate the answer to a specific question. As a result, this method clearly has the potential to positively affect the outcome of patients and has gained the status of "gold-standard" for the non-invasive evaluation of the acute abdomen over the last years, particularly after the developments in MDCT.

5. References

1. Tailored helical CT evaluation of acute abdomen. Radiographics. 2000 May-Jun;20(3):725-49.

2. Helical CT in the evaluation of the acute abdomen. AJR Am J Roentgenol. 2000 Apr;174(4):901-13.

3. Helical CT evaluation of acute right lower quadrant pain: part I, common mimics of appendicitis. AJR Am J Roentgenol. 2005 Apr;184(4):1136-42.

4. Helical CT evaluation of acute right lower quadrant pain: part II, uncommon mimics of appendicitis. AJR Am J Roentgenol. 2005 Apr;184(4):1143-9.

5. Multi-detector computed tomography of acute abdomen. Eur Radiol. 2005 Dec;15(12):2435-47.

6. Marincek B. Nontraumatic abdominal emergencies: acute abdominal pain: diagnostic strategies. Eur Radiol. 2002 Sep;12(9):2136-50.

7. CT of the acute abdomen: findings and impact on diagnosis and treatment. AJR Am J Roentgenol. 1994 Dec;163(6):1317-24.

8. CT of the acute abdomen: gynecologic etiologies. Abdom Imaging. 2003 May-Jun;28(3):416-32.

9. Impact of multislice CT on imaging of acute abdominal disease. Radiol Clin North Am. 2003 Nov;41(6):1083-93.

10. Mimics of renal colic: alternative diagnoses at unenhanced helical CT. Radiographics. 2004 Oct;24 Suppl 1:S11-28; discussion S28-33.

6. Author Information

figs orw.jpg

7. Mediafiles

figs orw.jpg

slide1.jpg

slide2.jpg

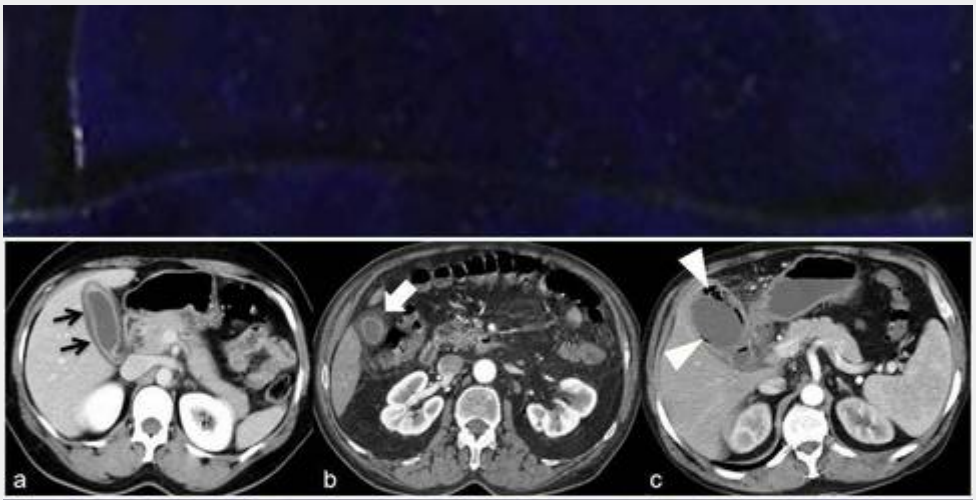

Fig. 2- Acute cholecystitis

a) Diffuse wall thickening of a distended gallbladder, which is surrounded by fluid (black arrows); **b)** Haziness of peri-cholecystic fat (white arrow); **c)** Intra-mural and intra-luminal gas (white arrowheads) in a case of emphysematous cholecystitis.

slide3.jpg

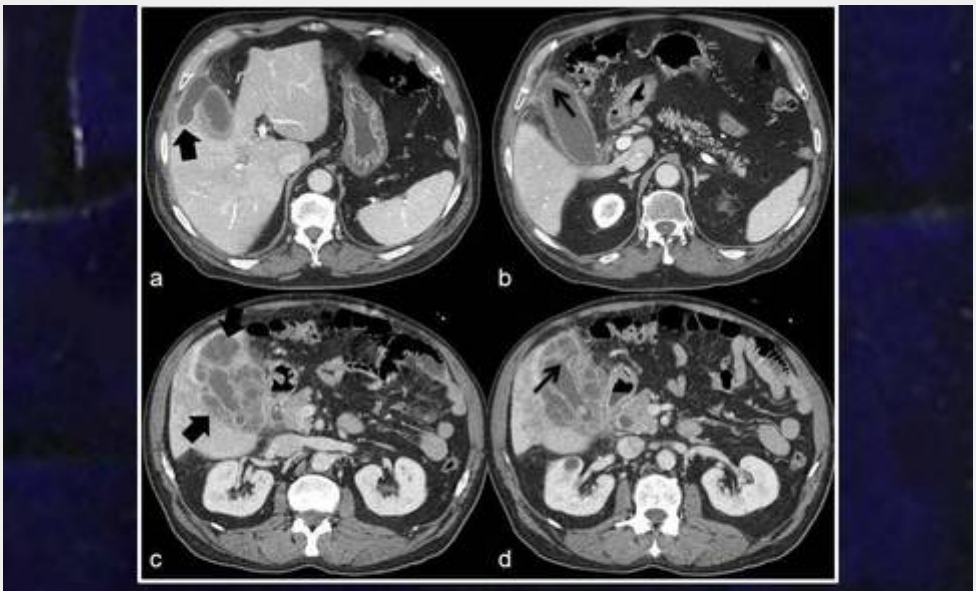

Fig. 3- Acute complicated cholecystitis

Two different cases of complicated cholecystitis (**a)** and **b)**; **c)** and **d)**) show perforation of the gallbladder wall (thin arrows on **b)** and **d)**) with formation of a pericholecystic abscess (thick arrows on **a)** and **c)**).

slide4.jpg

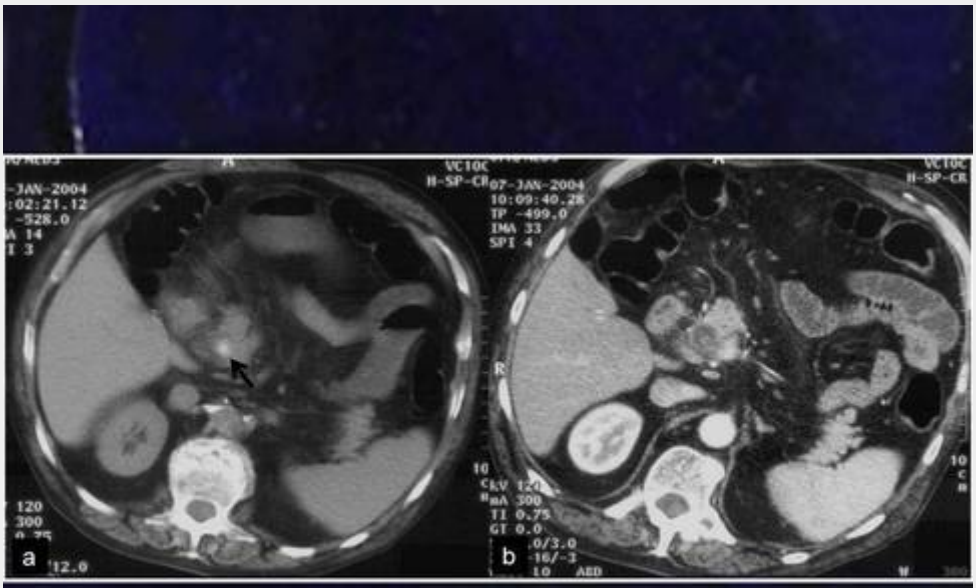

Fig. 4- Acute biliary colic

a) Non-enhanced CT clearly shows a spontaneous hyperdense stone located in the distal main biliary duct (black arrow); **b)** On contrast-enhanced CT the stone becomes much less visible, conveying the interest of obtaining plain scans in this setting; there is also dilatation of the main biliary duct with fluid.

slide5.jpg

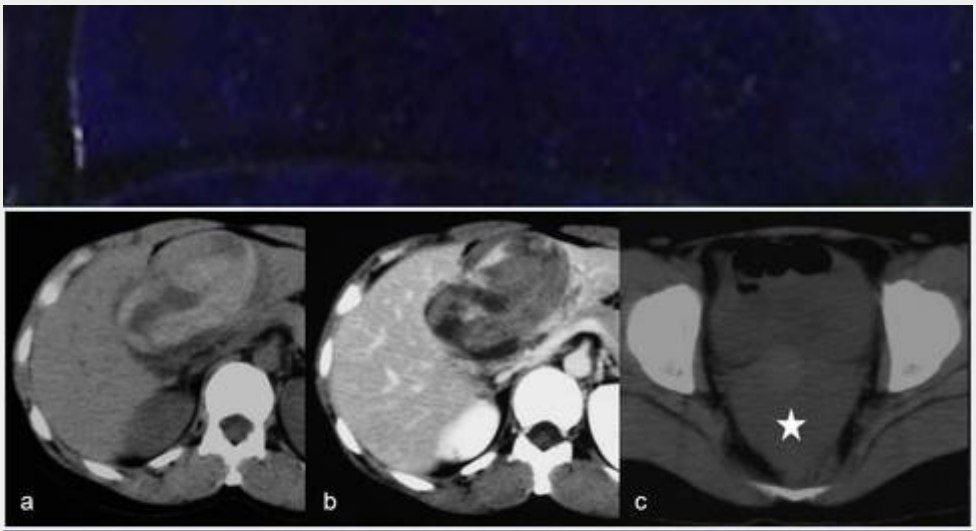

Fig. 5- Ruptured hepatic neoplasm

a) Non-enhanced CT demonstrates a spontaneous hyperdense liver mass corresponding to a haemorrhagic hepatocellular adenoma; **b)** On contrast-enhanced CT the focal liver lesion shows some heterogeneous enhancement but less than that of the adjacent parenchyma; **c)** Non-enhanced pelvic scan depicts a moderate amount of slightly hyperdense (haemorrhagic) fluid (white star).

slide6.jpg

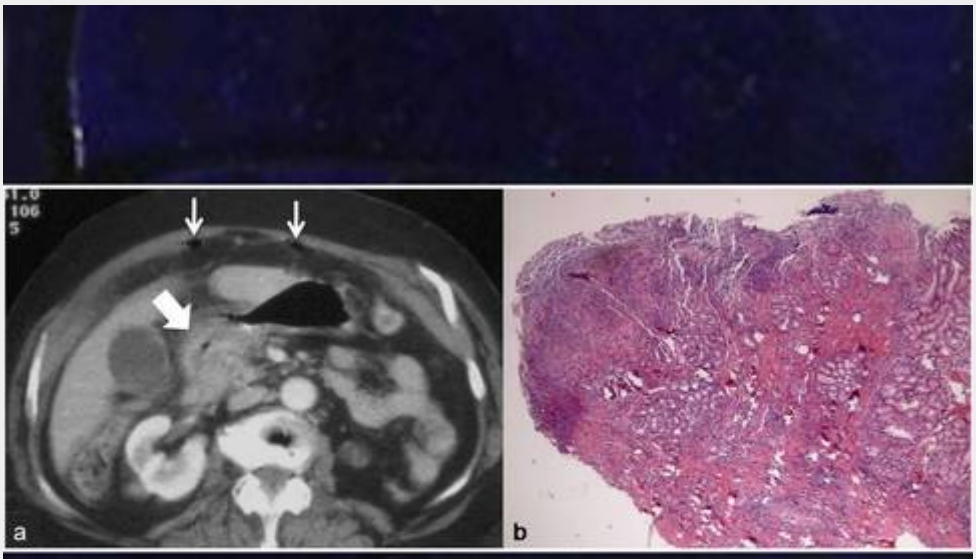

Fig. 6- Perforated peptic duodenal ulcer

a) Contrast-enhanced CT shows parietal thickening of the duodenal bulb (thick arrow) and small amounts of intra-peritoneal gas (thin arrows); **b)** Histology (H&E, 50x) shows inflammatory changes with granulation tissue and necrosis corresponding to the margins of the perforation.

slide7.jpg

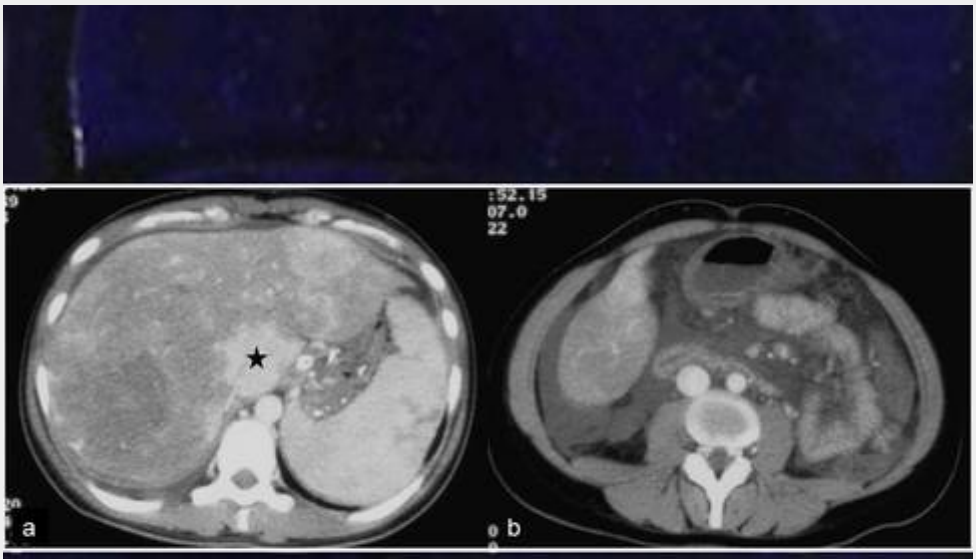

Fig. 7- Acute Budd-Chiari syndrome

a) Contrast-enhanced CT depicts a moderately enlarged liver with characteristic patchy enhancement and sparing of the caudate lobe (black star), and also a small amount of peritoneal fluid, which is much more evident on **b)**.

slide8.jpg

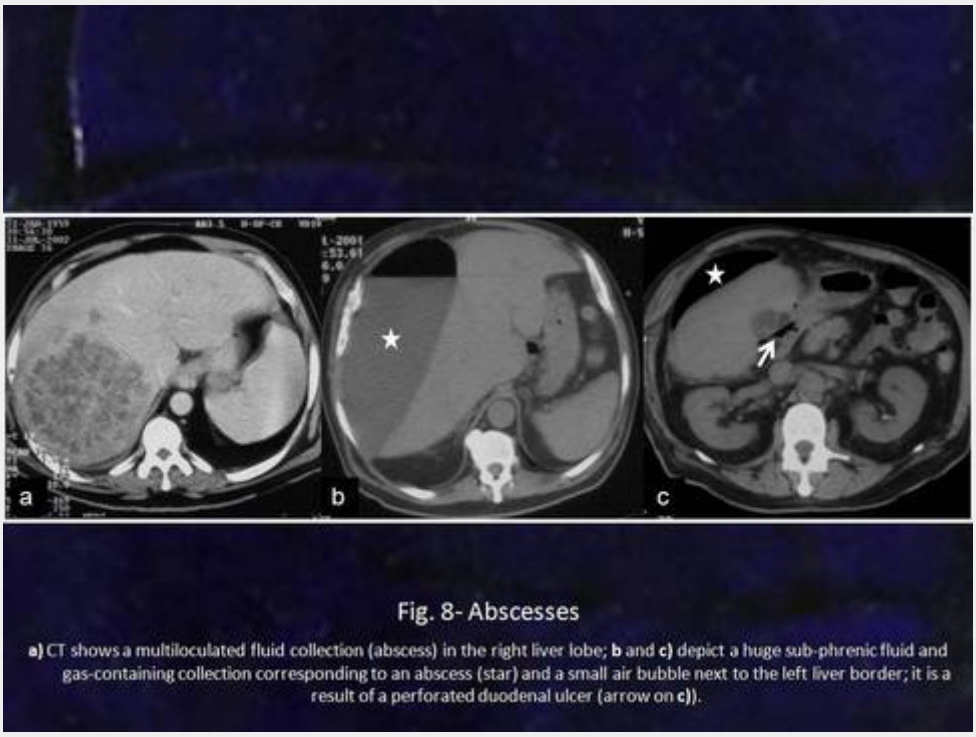

Fig. 8- Abscesses

a) CT shows a multiloculated fluid collection (abscess) in the right liver lobe; **b** and **c)** depict a huge sub-phrenic fluid and gas-containing collection corresponding to an abscess (star) and a small air bubble next to the left liver border; it is a result of a perforated duodenal ulcer (arrow on **c)**).

slide9.jpg

slide10.jpg

Fig. 10- Splenic infarctions

Contrast-enhanced CT shows hypodense areas in the splenic parenchyma of a patient with a haematological disorder presenting with acute left upper quadrant pain.

slide11.jpg

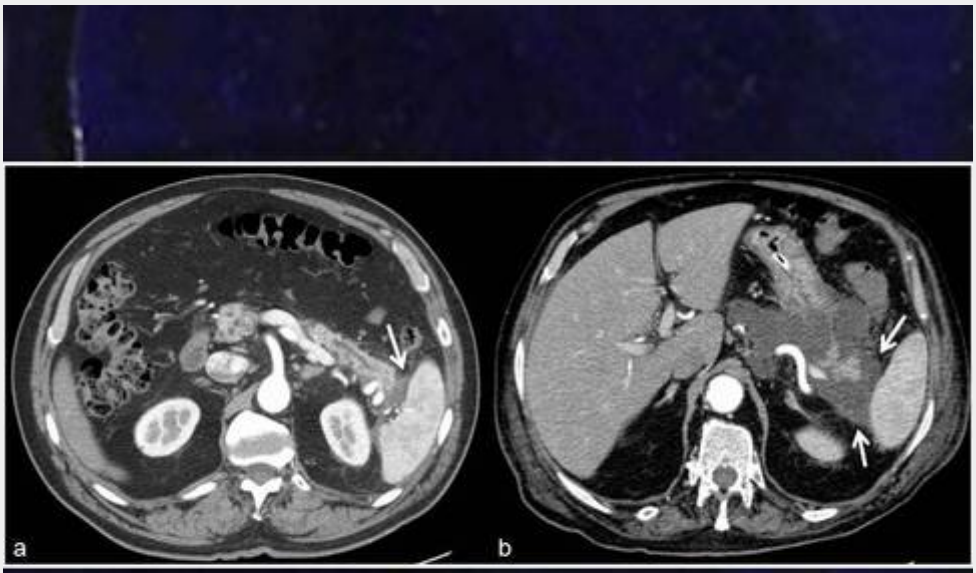

Fig. 11- Acute pancreatitis

a) and **b)** Contrast-enhanced CT images depict peri-pancreatic fluid collections abutting the surface of the spleen (arrows).

slide12.jpg

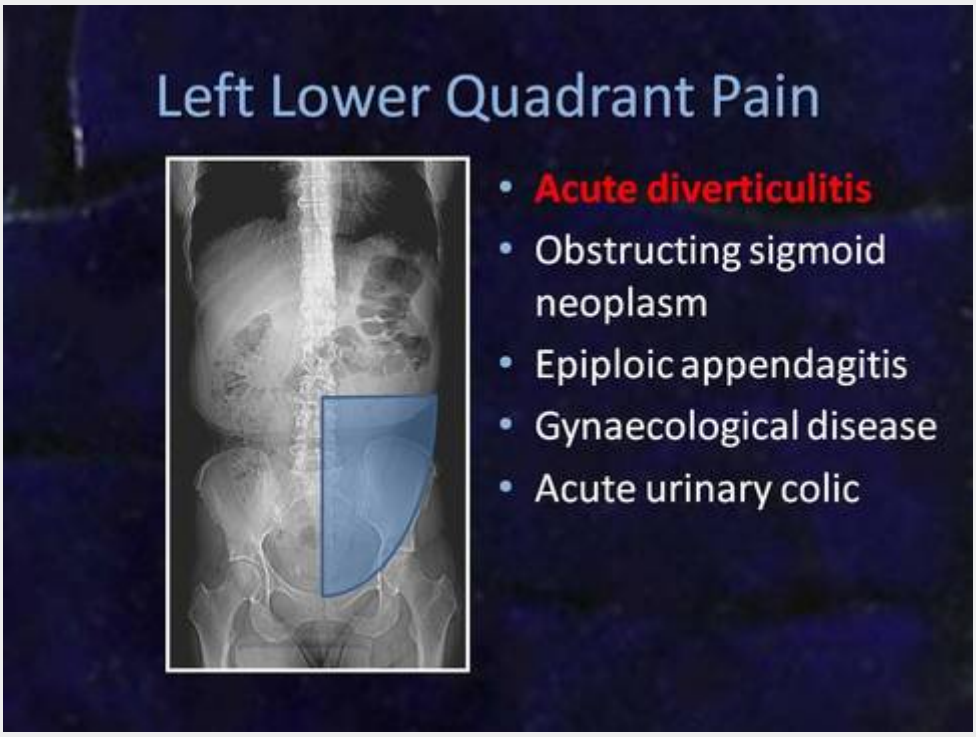

slide13.jpg

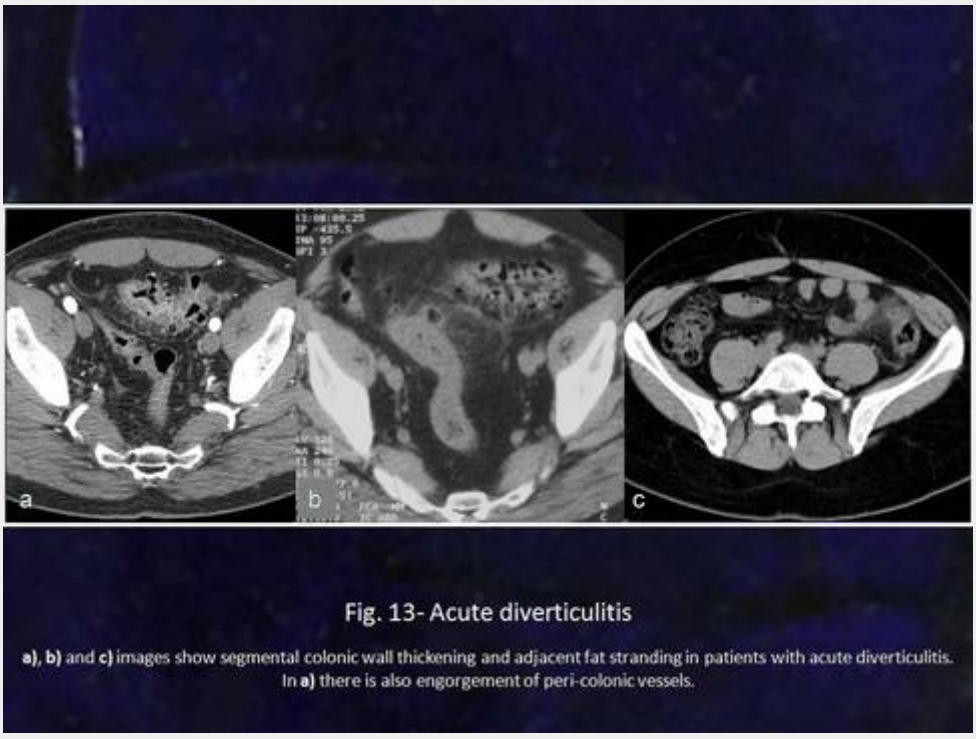

slide14.jpg

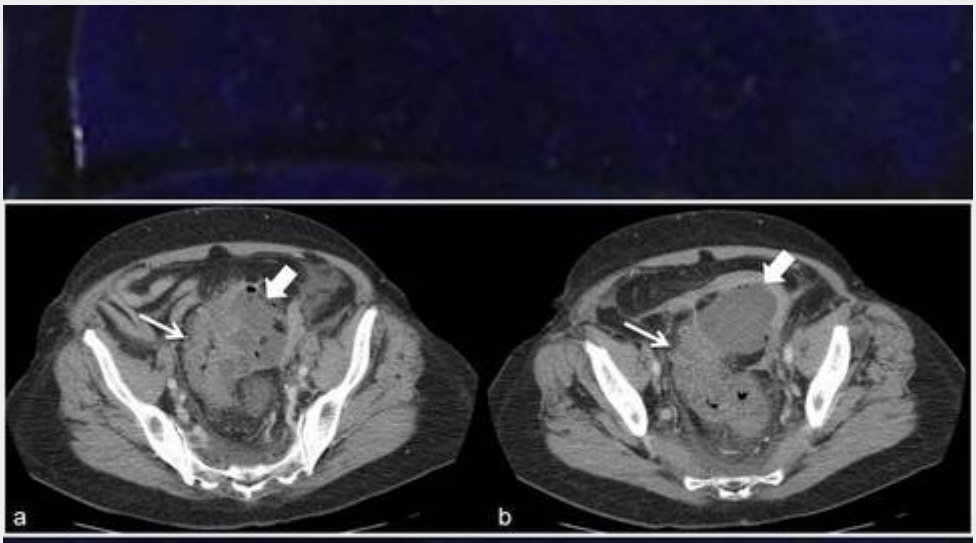

Fig. 14- Complicated acute diverticulitis

a) and **b)** Contrast-enhanced CT images depict thickening of the sigmoid wall (thin arrows) and adjacent fat stranding in a patient with acute diverticulitis complicated by a peri-colonic abscess containing small gas bubbles (thick arrows).

slide15.jpg

Fig. 15- Epiploic appendagitis

CT image reveals a lesion adjacent to the sigmoid colon (arrow) consisting of a fatty centre and a soft-tissue density rim at the periphery.

slide16.jpg

Fig. 16- Gynaecological disease

A cyst in the left adnexal region is shown by this CT image; it has a heterogeneous content with a fluid-fluid level, indicating the presence of internal haemorrhage.

slide17.jpg

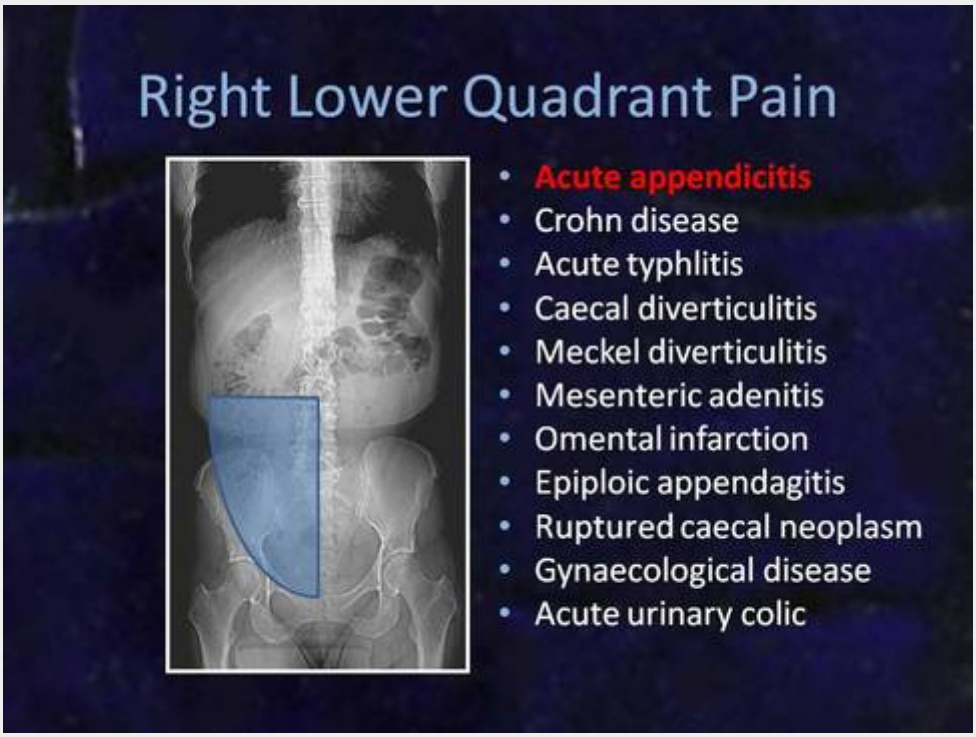

slide18.jpg

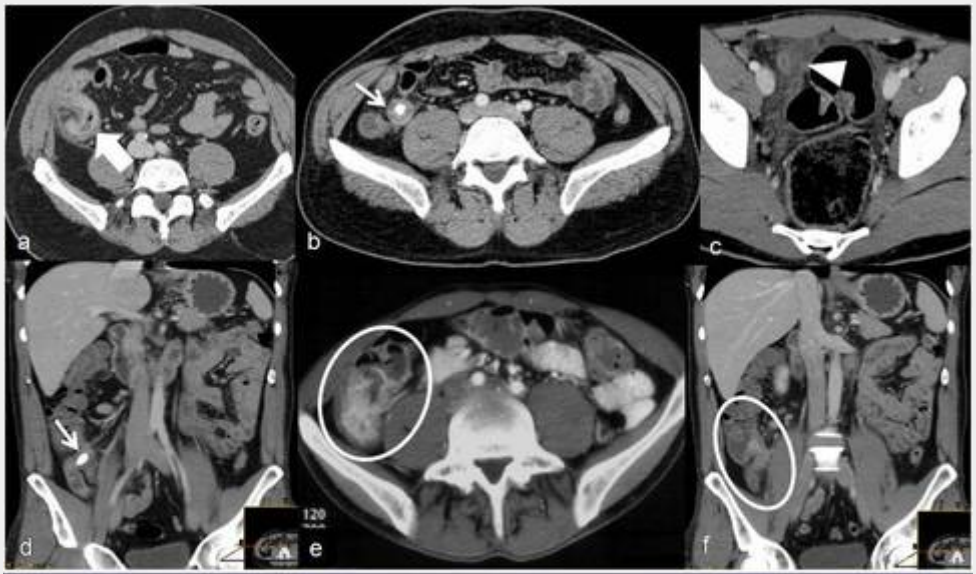

Fig. 18- Acute appendicitis

a) An enlarged, fluid-filled appendix with enhancement of the thickened wall and adjacent fat stranding (thick arrow) is shown; **b)** CT discloses a thick-walled appendix containing an appendicolith (thin arrow); **c)** there is a small quantity of fluid surrounding the inflamed appendix (arrowhead); **d)** a calcified appendicolith is seen within the appendiceal lumen (thin arrow); **e)** and **f)** images reveal focal caecal wall thickening (ellipses).

slide19.jpg

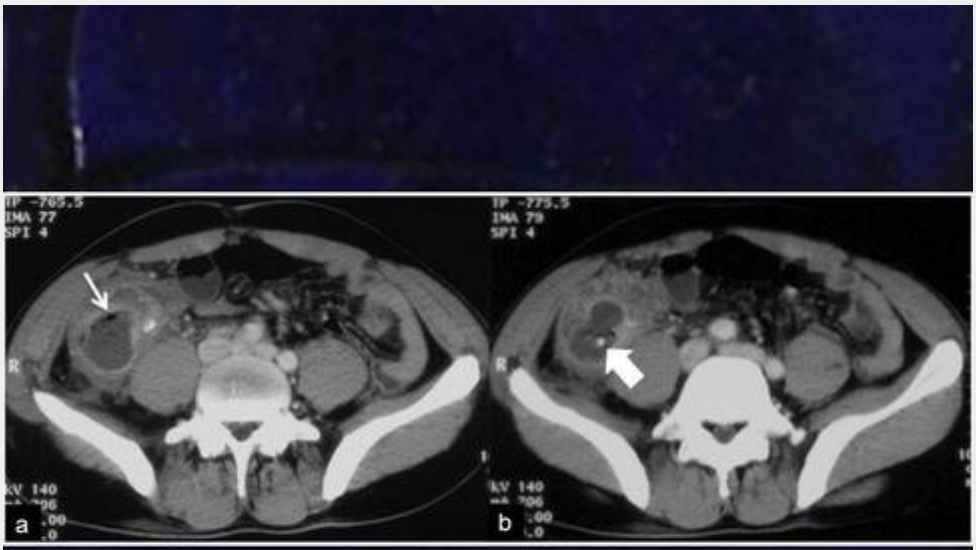

Fig. 19- Complicated acute appendicitis

a) and **b)** Contrast-enhanced CT images disclose a thick-walled fluid collection containing small gas bubbles (thin arrow on **a)**) and also calcified appendicoliths (thick arrow on **b)**), corresponding to an appendiceal abscess .

slide20.jpg

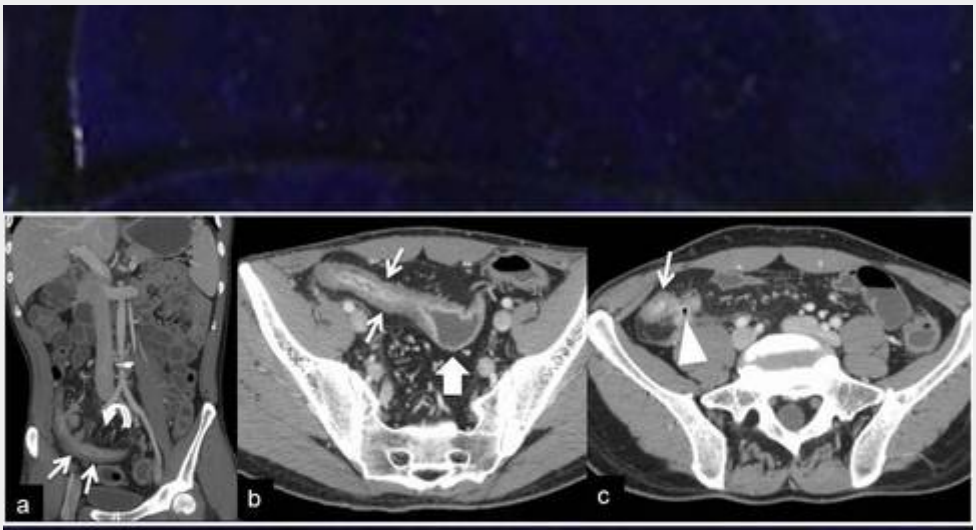

Fig. 20- Ileal Crohn disease

a), b) and **b)** Contrast-enhanced CT images reveal several thick-walled ileal loops with mucosal enhancement (thin arrows) consistent with active Crohn disease. Mesenteric hypervascularity (the "comb sign", curved arrow on **a)**) and spared segments are also noted (thick arrow on **b)**), as well as a small sinus tract (arrowhead on **c)**).

slide21.jpg

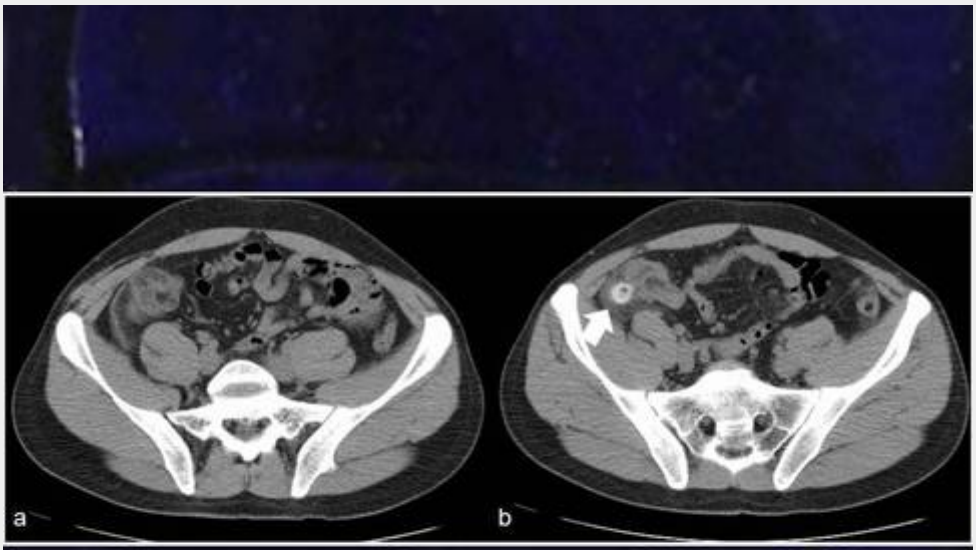

Fig. 21- Caecal diverticulitis

a) and **b)** CT images show segmental caecal wall thickening and adjacent fat stranding in a patient with acute diverticulitis. In **b)** there is also an impacted diverticulum (arrow).

slide22.jpg

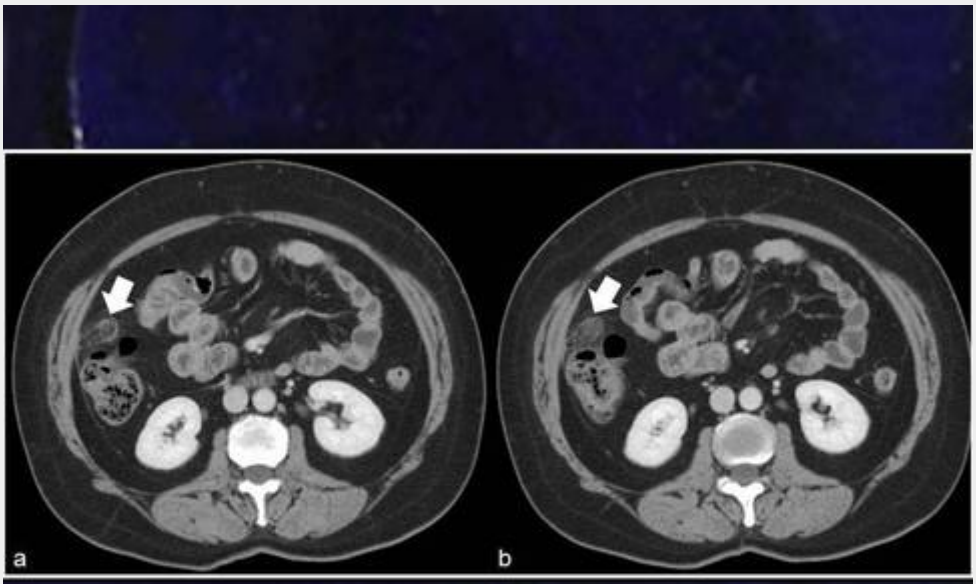

Fig. 22- Epiploic appendagitis

a) and **b)** images reveal a rounded mass adjacent to the ascending colon (arrows) displaying a central density of fat and a denser peripheral rim.

slide23.jpg

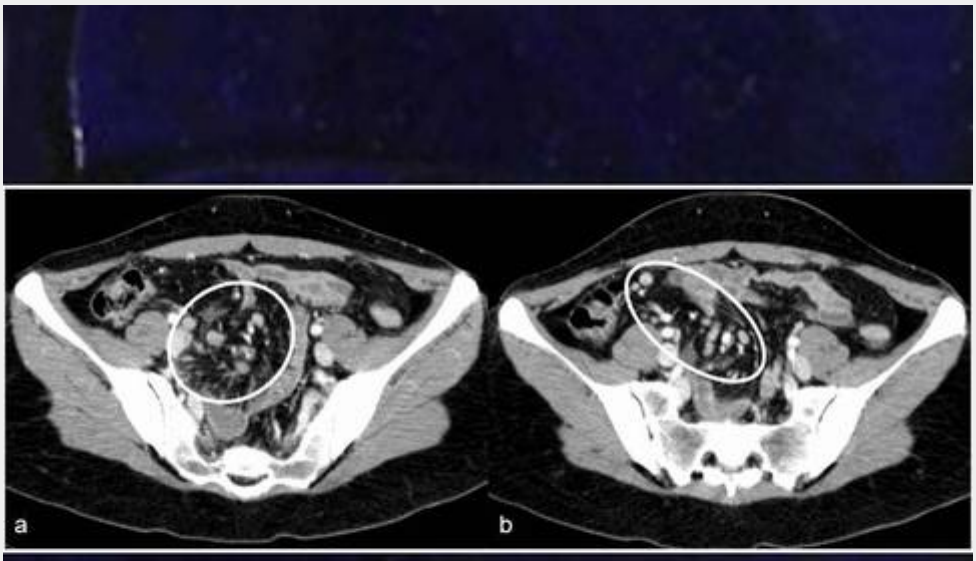

Fig. 23- Mesenteric adenitis

a) and **b)** images depict several enlarged mesenteric lymph nodes in a young patient with acute right lower quadrant pain, in the absence of other detectable abnormalities.

slide24.jpg

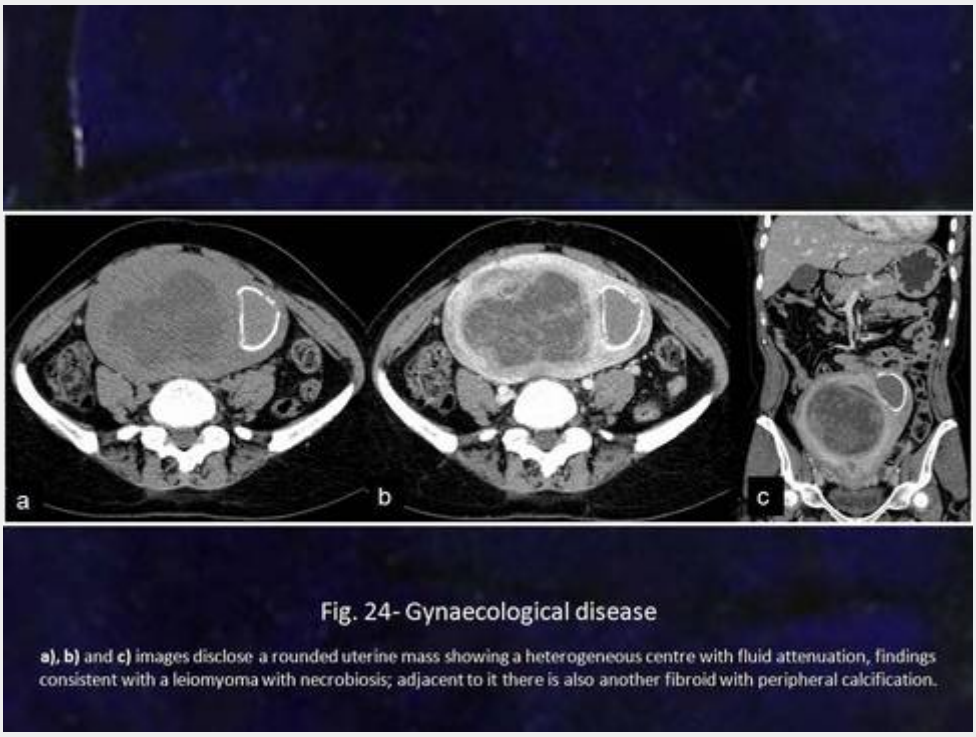

Fig. 24- Gynaecological disease

a), b) and **c)** images disclose a rounded uterine mass showing a heterogeneous centre with fluid attenuation, findings consistent with a leiomyoma with necrobiosis; adjacent to it there is also another fibroid with peripheral calcification.

slide25.jpg

slide26.jpg

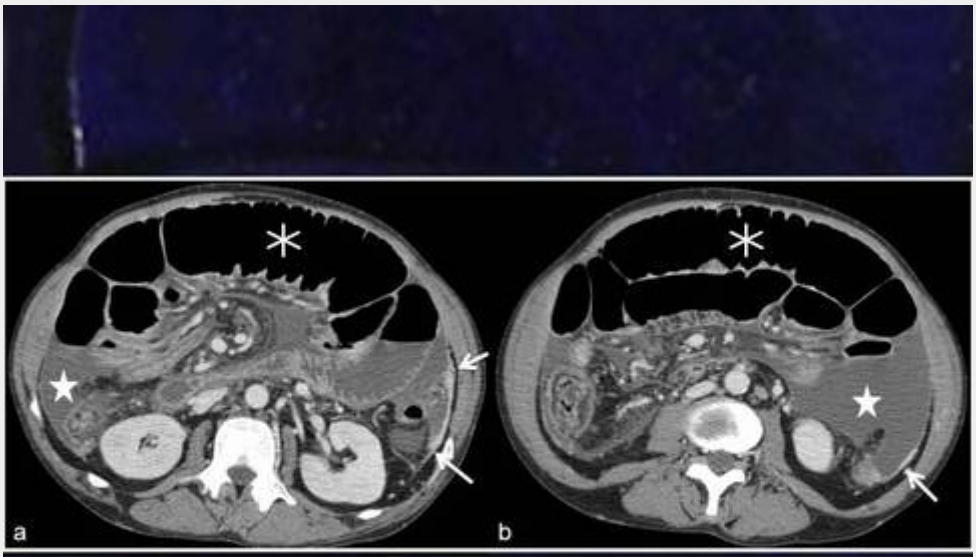

Fig. 26- Paralytic ileus secondary to spontaneous bacterial peritonitis

a) and **b)** CT images show several enlarged small bowel loops (asterisks) in a patient with spontaneous bacterial peritonitis manifesting as peritoneal fluid (star), thickening and enhancement (arrows).

slide27.jpg

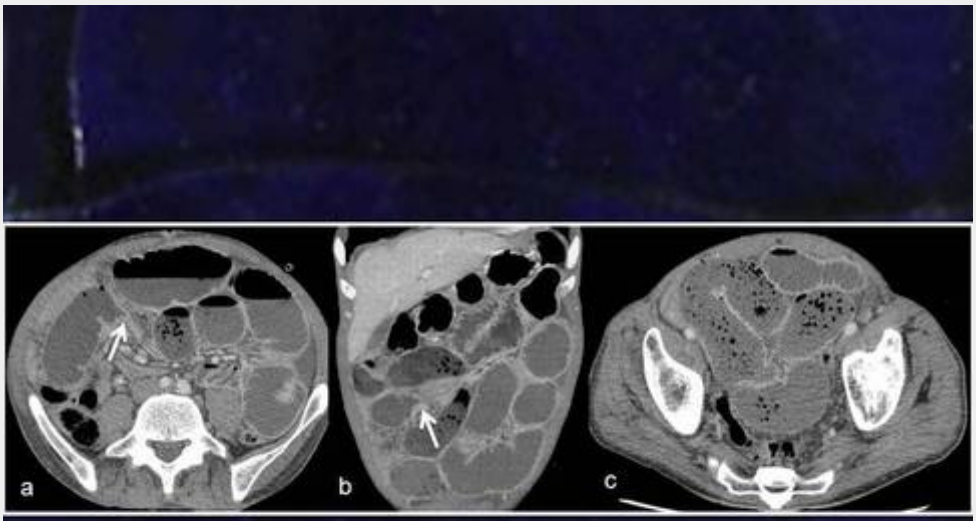

Fig. 27- Small bowel obstruction caused by an adhesion

Contrast-enhanced CT images depict signs of a SBO obstruction due to an adhesion, surgically confirmed. There is an abrupt transition zone (arrows on **a)** and **b)**) in the absence of a detectable organic lesion. The proximal bowel is distended with fluid and tiny air bubbles (**c)**), an appearance similar to faecal content ("small bowel faeces sign").

slide28.jpg

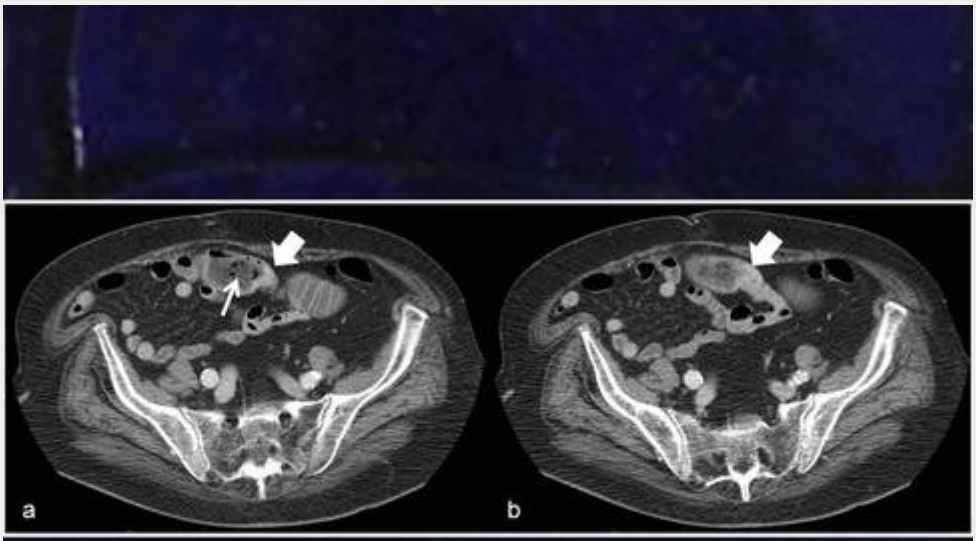

Fig. 28- Small bowel obstruction due to a jejunal adenocarcinoma

a) and **b)** An abrupt transition zone from the distended to the decompressed jejunum due to an adenocarcinoma manifesting also as a thickening of the bowel wall (thick arrows) is seen. The proximal bowel is distended with fluid mixed with tiny air bubbles (thin arrow on **a)**), resembling faecal content (the "small bowel faeces sign").

slide29.jpg

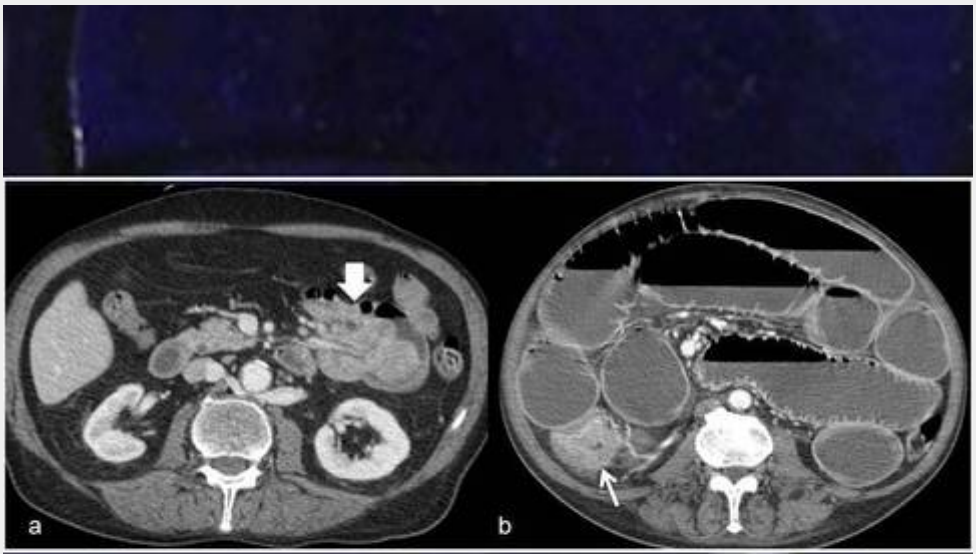

Fig. 29- Small bowel obstruction caused by neoplasm

a) In a patient with low-grade obstruction, CT depicts a small bowel neoplasm causing an intussusception (thick arrow); **b)** This high-grade obstruction is caused by a proximal colonic adenocarcinoma manifesting as bowel wall thickening (thin arrow). The proximal bowel is markedly distended with fluid and gas.

slide30.jpg

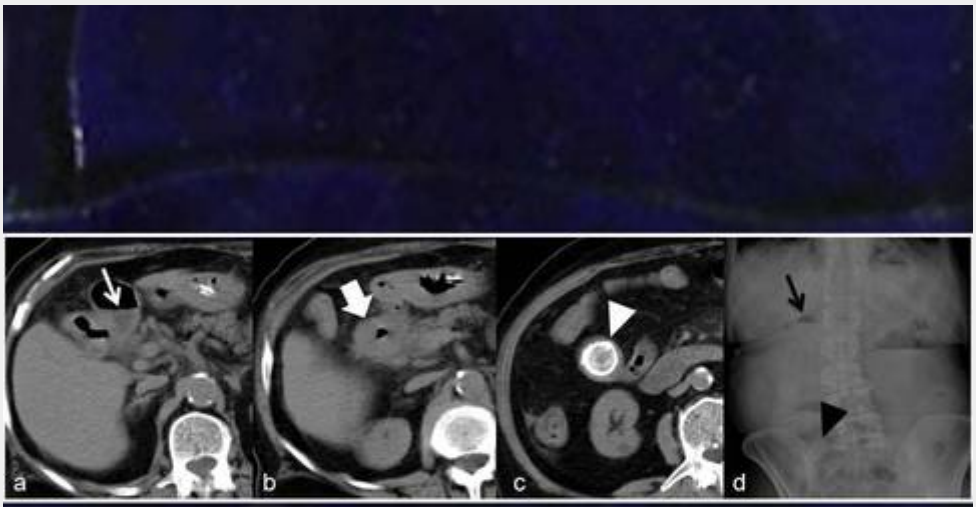

Fig. 30- Gallstone ileus

a) and **b)** CT images show an air-fluid level in the lumen of gallbladder (thin white arrow) and diffuse thickening of the duodenal wall (thick white arrow); **c)** A more caudal slice depicts a gallstone in the small bowel lumen (white arrowhead); **d)** Abdominal film also shows the air-fluid level in the gallbladder (thin black arrow) and the gallstone (black arrowhead).

slide31.jpg

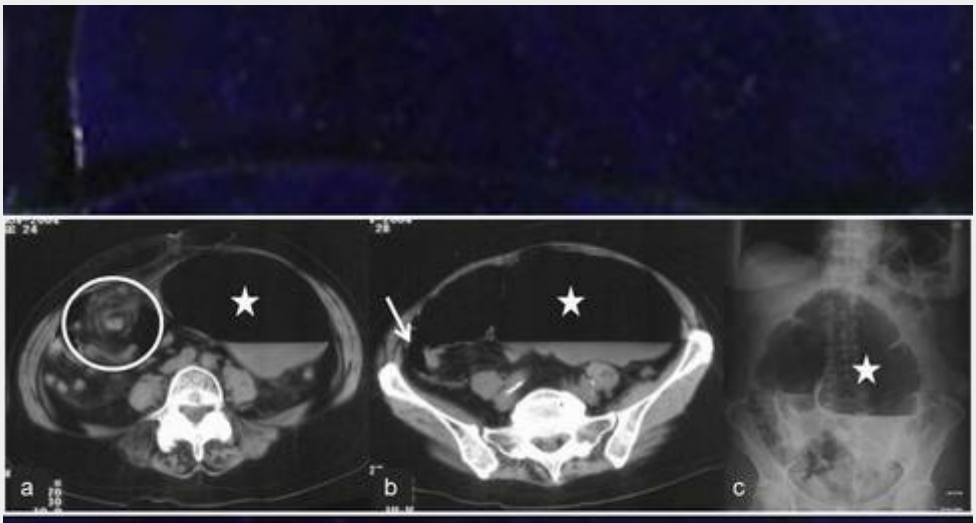

Fig. 31- Closed-loop LBO

a) and **b)** CT images depict a massively enlarged, gas and fluid-filled large bowel loop corresponding to a caecal volvulus (star); the diagnosis is also supported by a zone of twisting of the mesenteric vessels (white circle on **a)**) and a normally located ileo-caecal valve which however opens medially (arrow on **b)**); **c)** plain film shows an enlarged bowel loop with an air-fluid level, extending to the left abdominal quadrants.

slide32.jpg

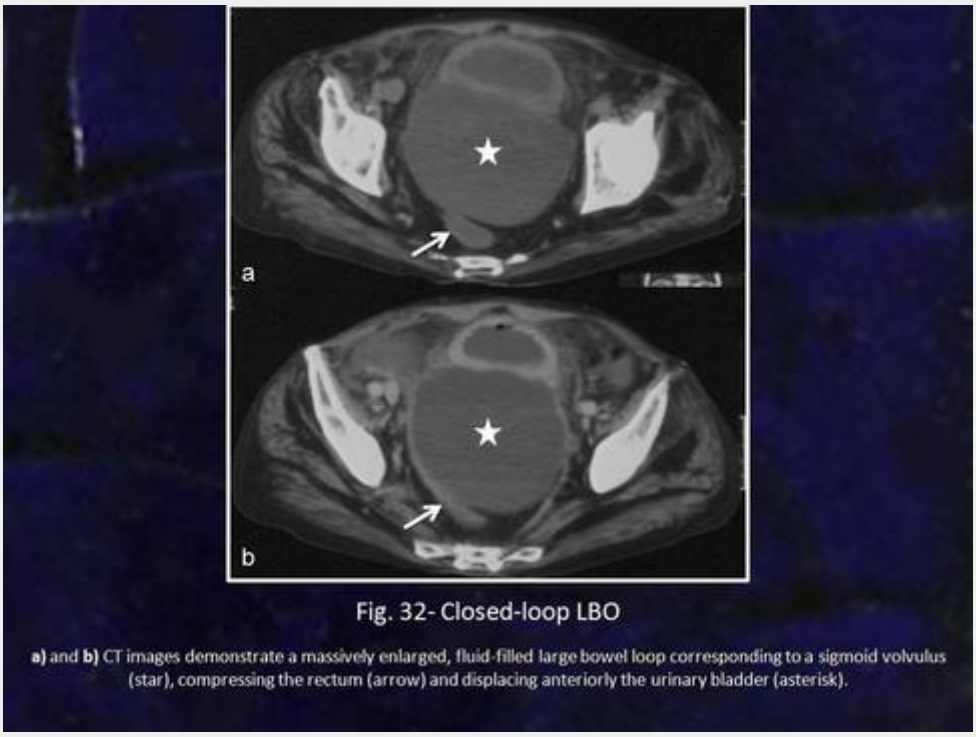

Fig. 32- Closed-loop LBO

a) and **b)** CT images demonstrate a massively enlarged, fluid-filled large bowel loop corresponding to a sigmoid volvulus (star), compressing the rectum (arrow) and displacing anteriorly the urinary bladder (asterisk).

slide33.jpg

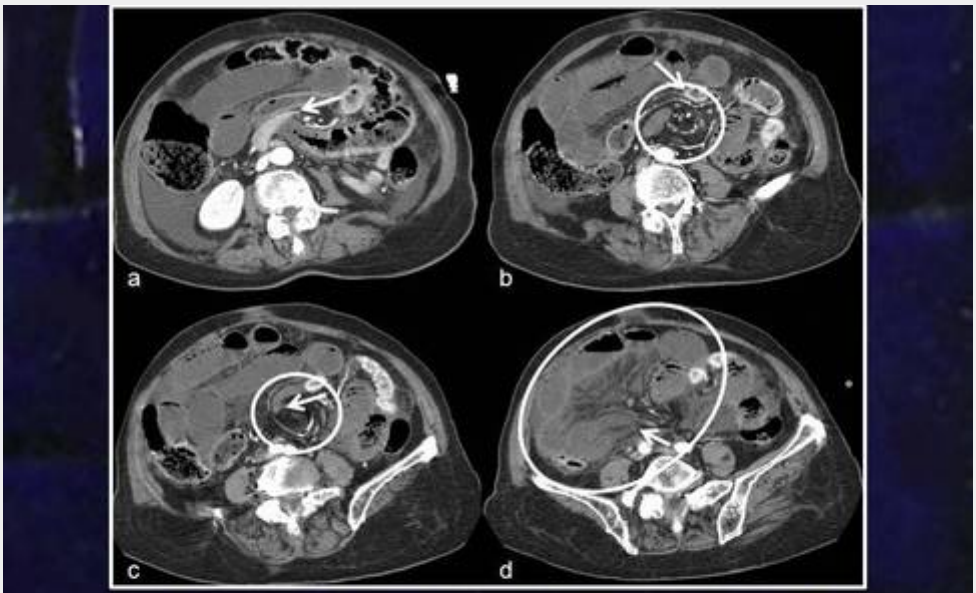

Fig. 33- Strangulated small bowel obstruction caused by an internal hernia

Contrast-enhanced CT images depict signs of a closed-loop obstruction due to a transmesenteric internal hernia, consisting of several beak-shaped SBO loops (arrows) and twisting of the mesenteric vessels (the "whirl sign", circles on **b)** and **c)**). There is also evidence of strangulation: non-enhancement of the thickened wall of several bowel loops to where engorged mesenteric vessels converge, mesenteric oedema/ haemorrhage, ascites (ellipse on **d)**).

slide34.jpg

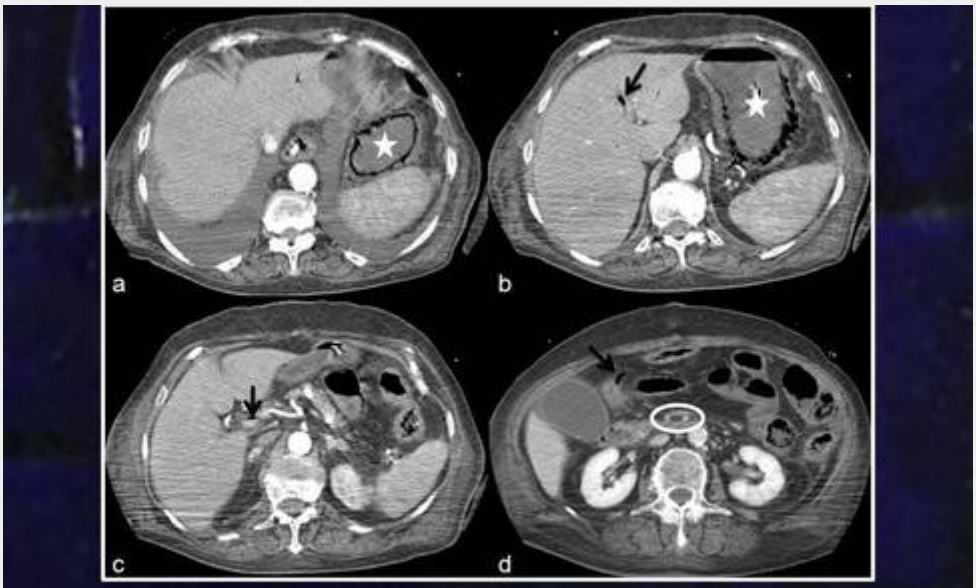

Fig. 34- Acute ischemia due to hypoperfusion

a) and **b)** Contrast-enhanced CT images demonstrate gastric wall pneumatosis (star); arrows on **b)**, **c)** and **d)** indicate respectively gas in the intra-hepatic portal vein, in the portal main trunk and in a mesenteric vessel; there is patency of both the SMA and the SMV (circle on **d)**).

slide35.jpg

Fig. 35- Ischemic bowel disease

a) and **b)** Contrast-enhanced CT images demonstrate filling defects in the spleno-mesenteric confluent (arrow on **a)**) and in the SMV with normal patency of the SMA (circle on **b)**); **c)** and **d)** show several dilated small bowel loops with thickened, poorly-enhancing wall, as well as mesenteric oedema/ haemorrhage and ascites.

slide36.jpg

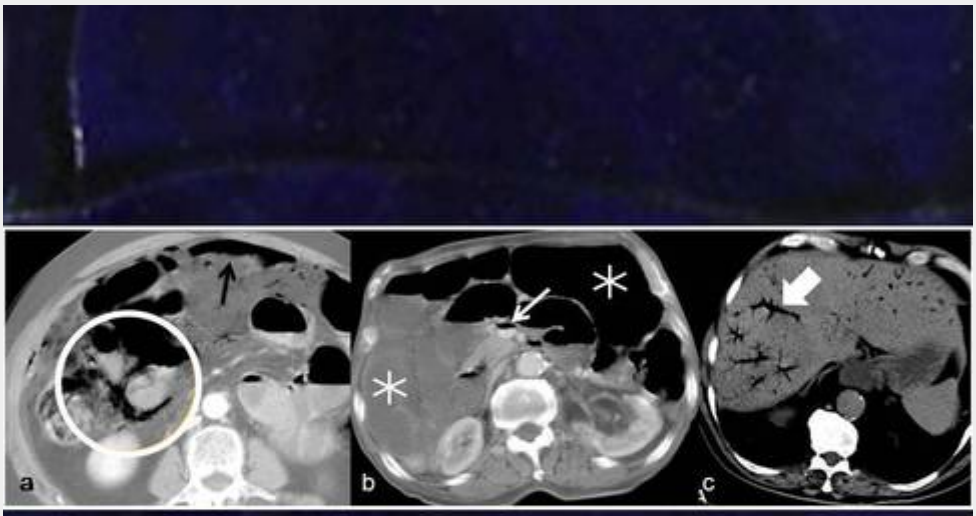

Fig. 36- Ischemic bowel disease

a) CT image demonstrate pneumatosis intestinalis (circle) and a small pneumoperitoneum (thin black arrow); thin white arrow on **b)** indicates gas in the SMV, as well as various dilated small bowel loops filled with gas and fluid (asterisks); **c)** CT image shows gas in the intra-hepatic portal vein branches (thick arrow). These findings are generally associated with a dismal prognosis.

slide37.jpg

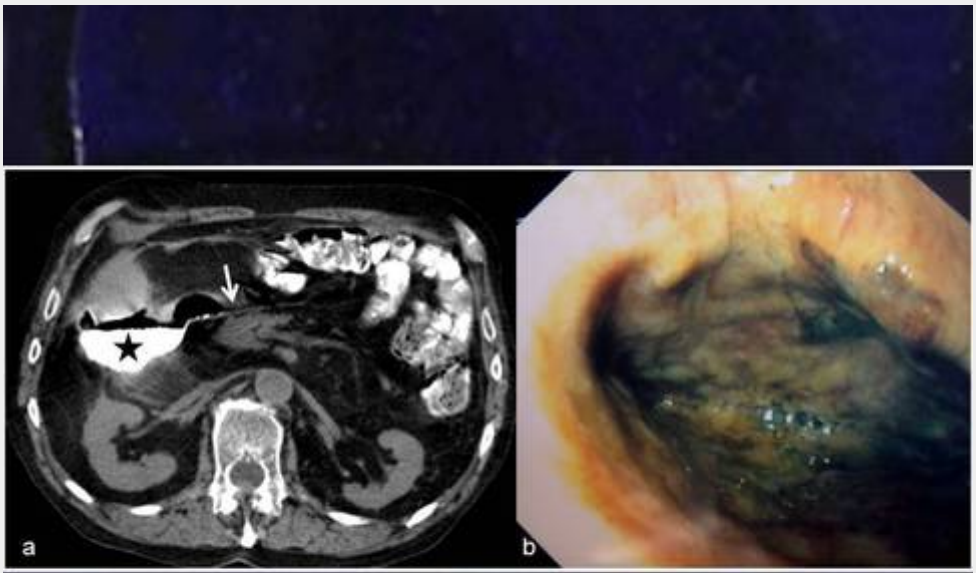

Fig. 37- Perforated peptic duodenal ulcer

a) Abdominal CT clearly shows the site of the duodenal perforation (arrow) and accumulation of gas and water-soluble positive oral contrast in the right anterior pararenal space (star); **b)** Endoscopy shows a large, deep, necrotic ulceration on the posterior wall of the duodenal bulb.

slide38.jpg

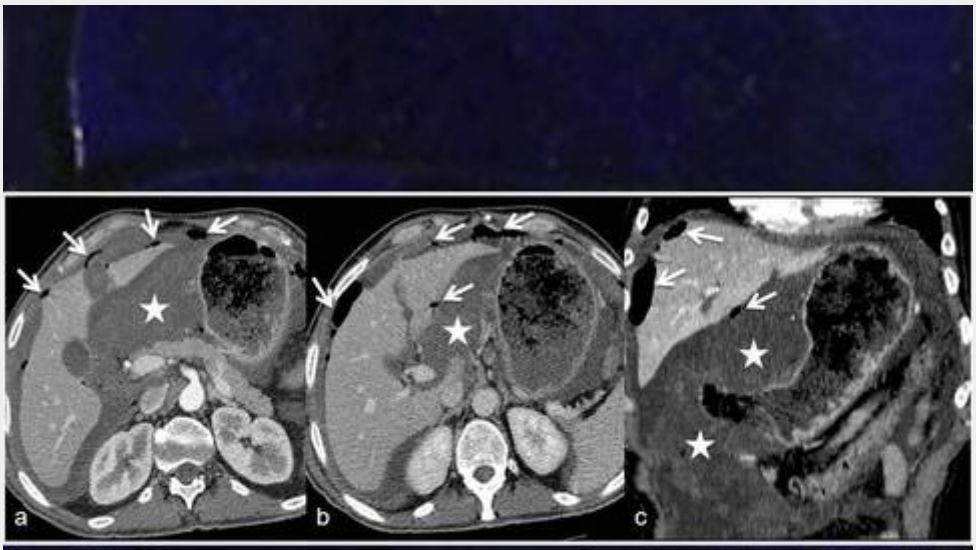

Fig. 38- Perforated gastric neoplasm

a), b) and **c)** images all demonstrate a huge heterogeneous gastric tumor (stars) which has ruptured and originated multiple pockets of intra-peritoneal gas (arrows). Note also the presence of abundant ascites.

slide39.jpg

Fig. 39- Duodenal perforation following ERCP with sphincterothomy for biliary lythiasis

a) and **b)** contrast-enhanced CT images performed with water-soluble positive oral contrast agent show retroperitoneal extravasation into the right anterior pararenal space (arrow) and abundant retroperitoneal gas. Note cholelythiasis, intra- and extra-hepatic aerobilia, and main pancreatic duct dilatation with severe atrophy of pancreatic parenchyma; **c)** and **d)** plain films reveal the extent of gas collections, with pneumoretroperitoneum and mediastinal, cervical, and subcutaneous emphysema.

slide40.jpg

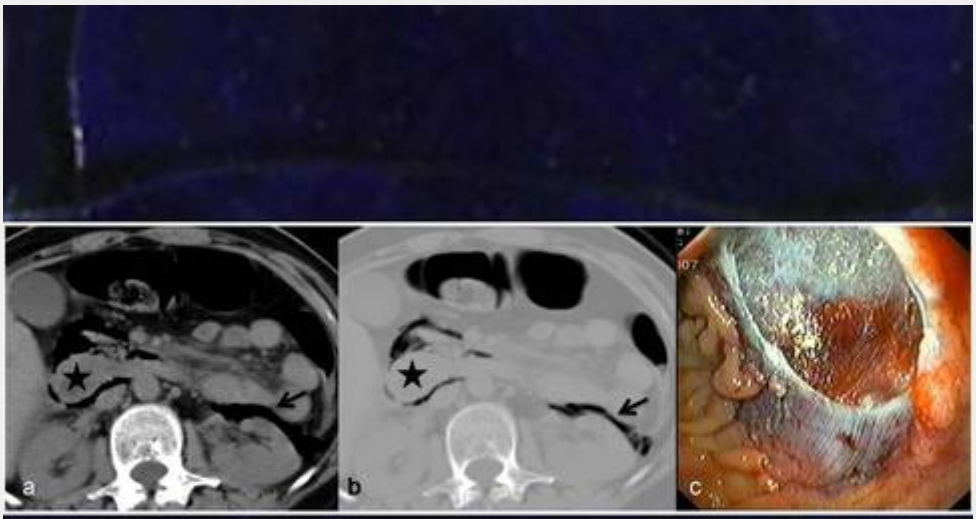

Fig. 40- Duodenal perforation secondary to endoscopic mucosectomy

a) and **b)** CT slices show gas surrounding the 2nd and 3rd portions of the duodenal loop (star) and in the left anterior pararenal space (arrow), best recognised on a lung window setting (**b)**); **c)** Post-mucosectomy endoscopic frame shows a large perforation, revealing retroperitoneal fascial planes; white clear-cut ulcer edges are due to thermal snare injury.

slide41.jpg

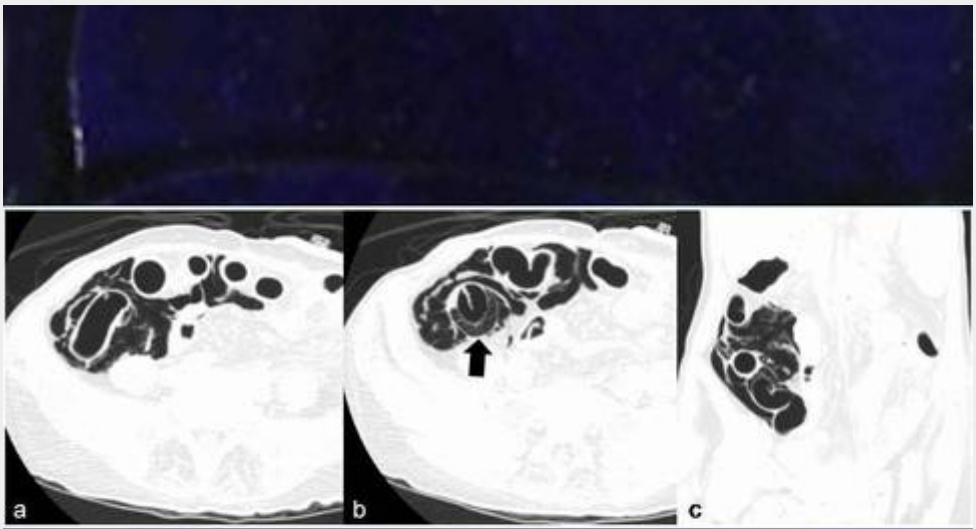

Fig. 41- Colonic perforation following optical colonoscopy

a), **b)** and **c)** CT images on a lung window setting all reveal abundant gas surrounding multiple bowel loops and also dissecting the colonic wall (arrow on **b)**).

slide42.jpg

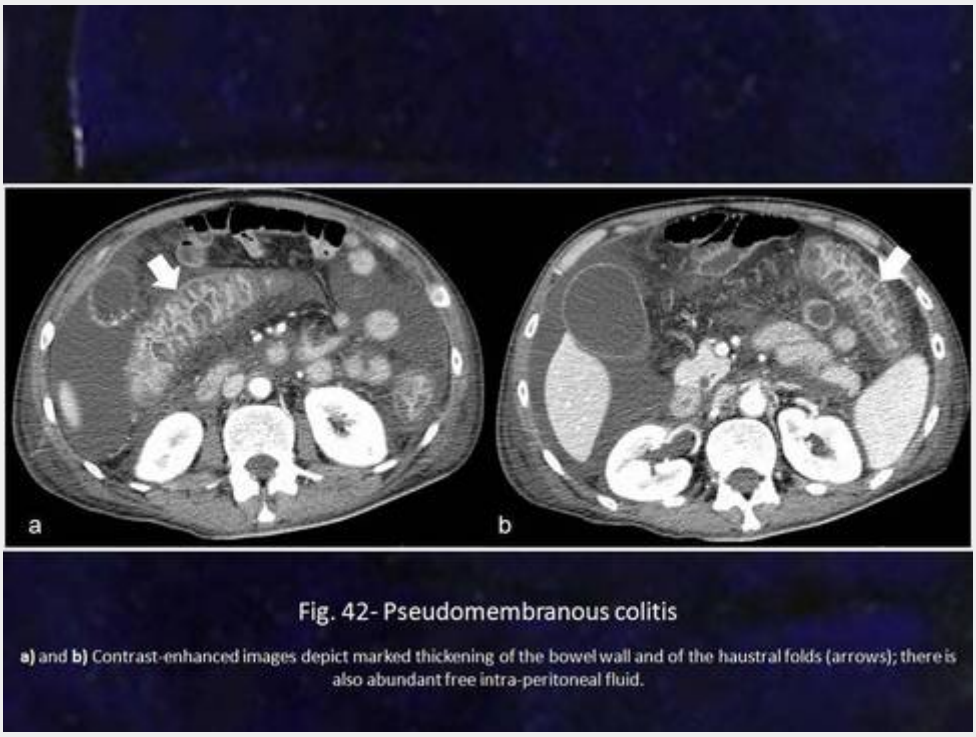

Fig. 42- Pseudomembranous colitis

a) and **b)** Contrast-enhanced images depict marked thickening of the bowel wall and of the haustral folds (arrows); there is also abundant free intra-peritoneal fluid.

slide43.jpg

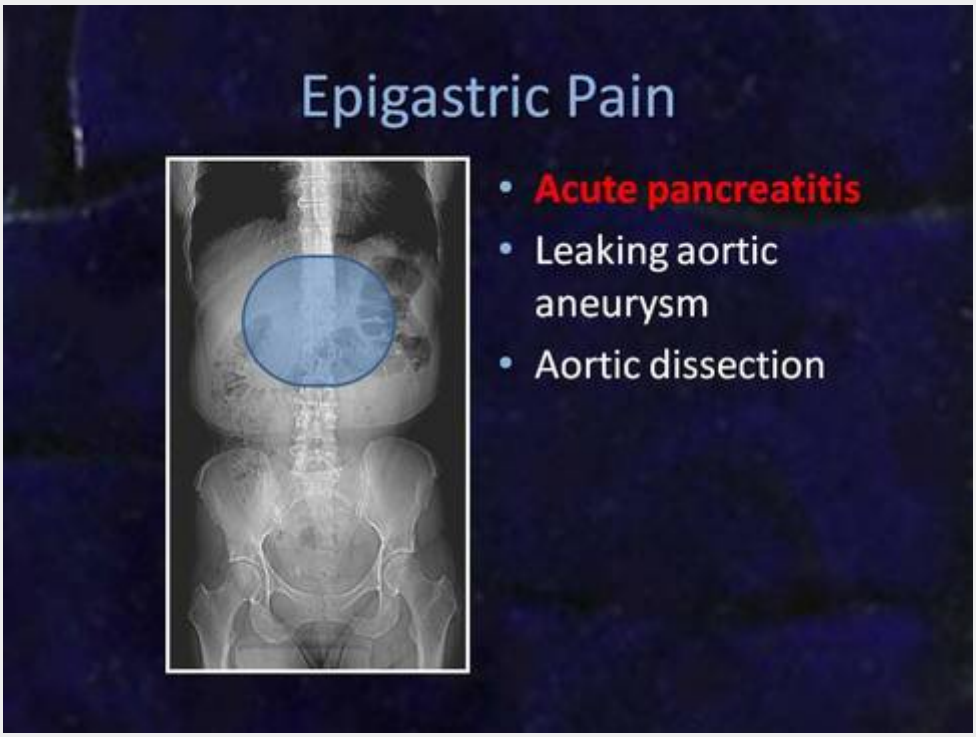

slide44.jpg

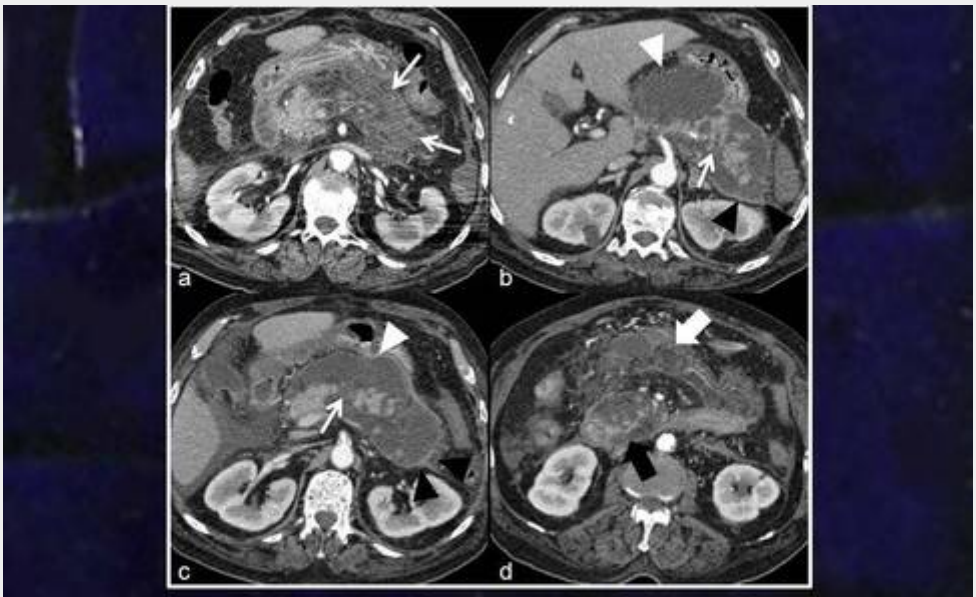

Fig. 44- Acute pancreatitis

Contrast-enhanced studies show parenchymal areas with absent enhancement, corresponding to necrotic parenchyma (thin arrows on **a)**, **b)** and **c)**). There are also peri-pancreatic fluid collections in different locations: lesser sac (white arrowheads), anterior para-renal space (black arrowheads), mesenteric root (thick black arrow) and transverse mesocolon (thick white arrow).

slide45.jpg

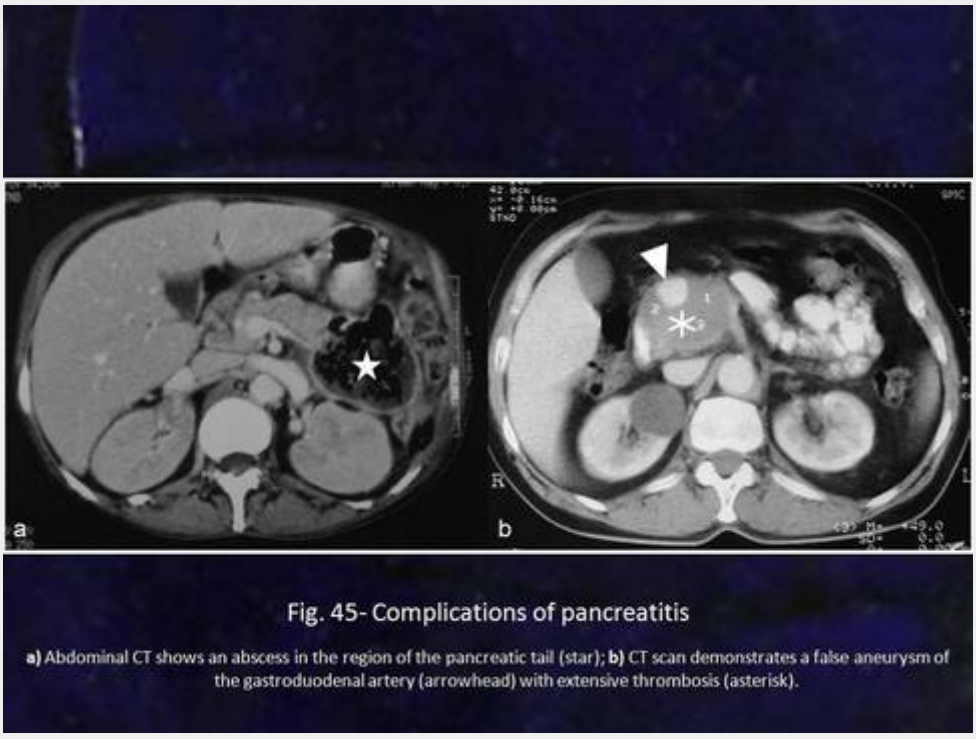

Fig. 45- Complications of pancreatitis

a) Abdominal CT shows an abscess in the region of the pancreatic tail (star); **b)** CT scan demonstrates a false aneurysm of the gastroduodenal artery (arrowhead) with extensive thrombosis (asterisk).

slide46.jpg

Fig. 46- Aortic dissection

a) and **b)** CT images show complex aortic dissections, involving the celiac trunk (**a)**) and the SMA (**b)**).

slide47.jpg

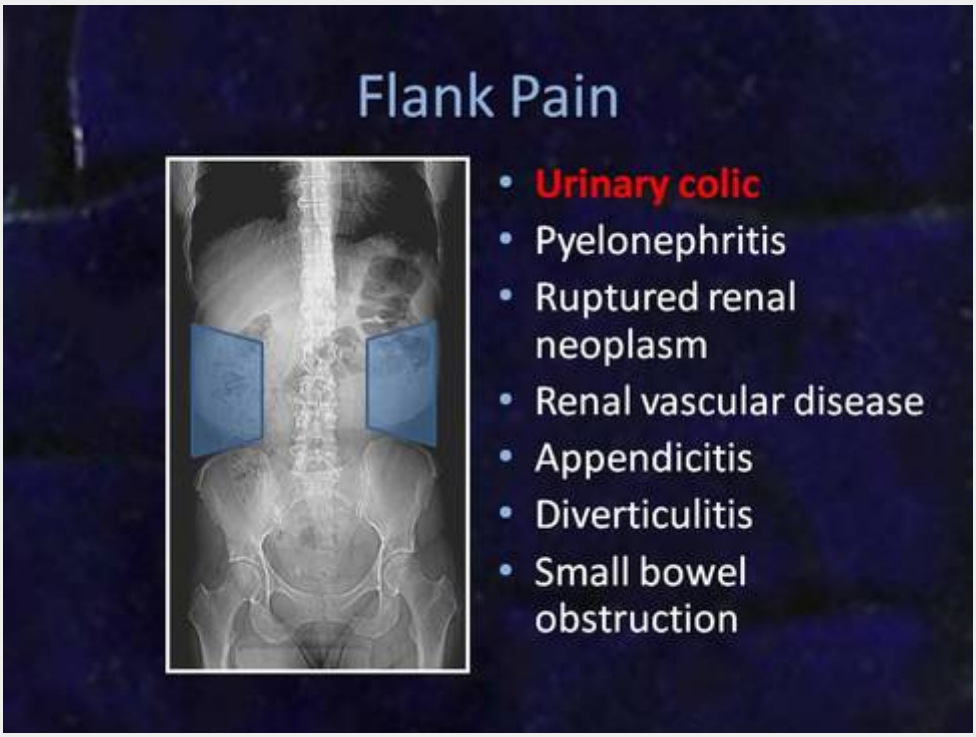

slide48.jpg

Fig. 48- Acute urinary colic

a) Non-enhanced CT depicts a dilated right renal pelvis (thick arrow); **b)** CT shows dilatation of the right ureter (arrowhead); **c)** CT image demonstrates a stone in the lower third of the ureter associated with peri-ureteral fat stranding (circle); **d)** CT reveals an urinary stone in the uretero-vesical junction (thin arrow).

slide49.jpg

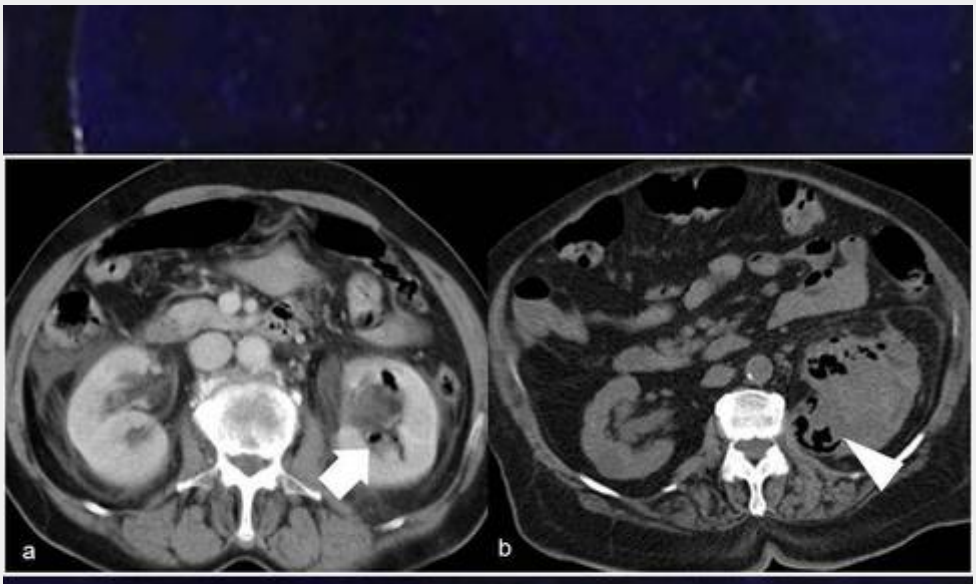

Fig. 49- Acute renal infection

a) Abdominal contrast-enhanced CT shows gas in the collecting system of the left kidney, corresponding to an emphysematous pyelitis (arrow); **b)** CT scan demonstrates parenchymal gas, characteristic of an emphysematous pyelonephritis (arrowhead).

slide50.jpg

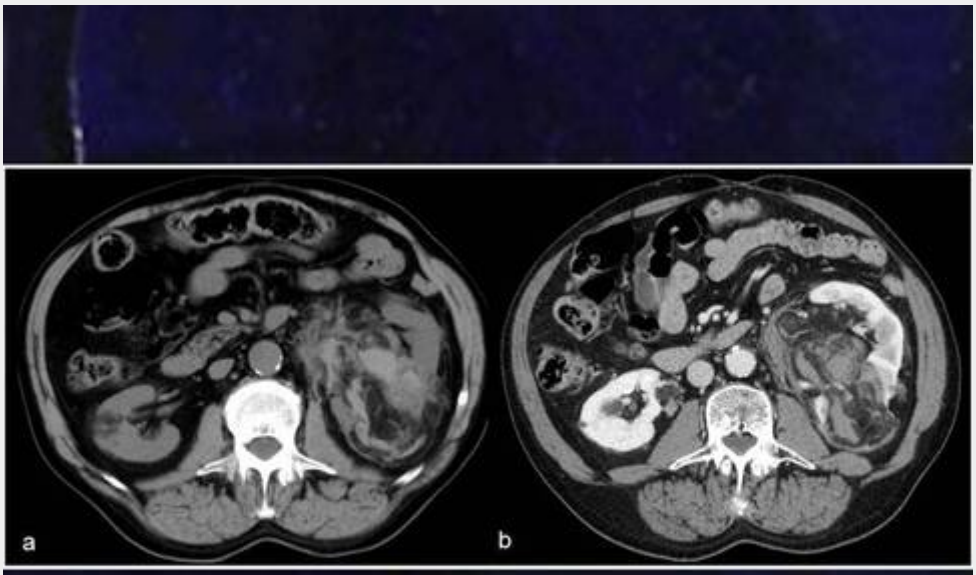

Fig. 50- Ruptured renal neoplasm

a) and **b)** CT slices demonstrate a predominantly fatty left renal mass with spontaneous hyperdense areas corresponding to a haemorrhagic angiomyolipoma. Note the presence of other angiomyolipomas in the opposite kidney.

slide51.jpg

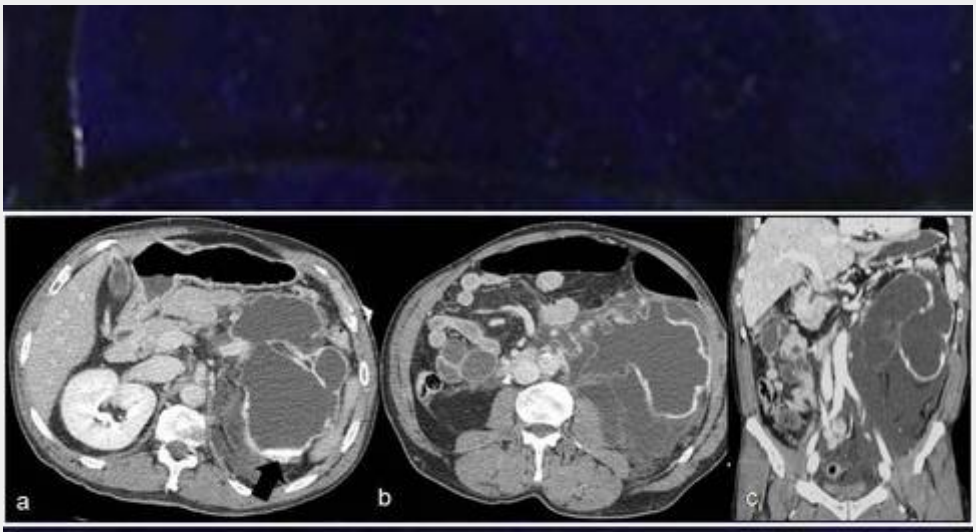

Fig. 51- Ruptured hydronephrotic kidney

a), b) and **c)** images demonstrate signs of rupture of a markedly hydronephrotic left kidney, represented by extensive retroperitoneal fluid outside the collecting system; there is contrast layering inside the dilated collecting system indicated by an arrow in **a)**.

slide52.jpg

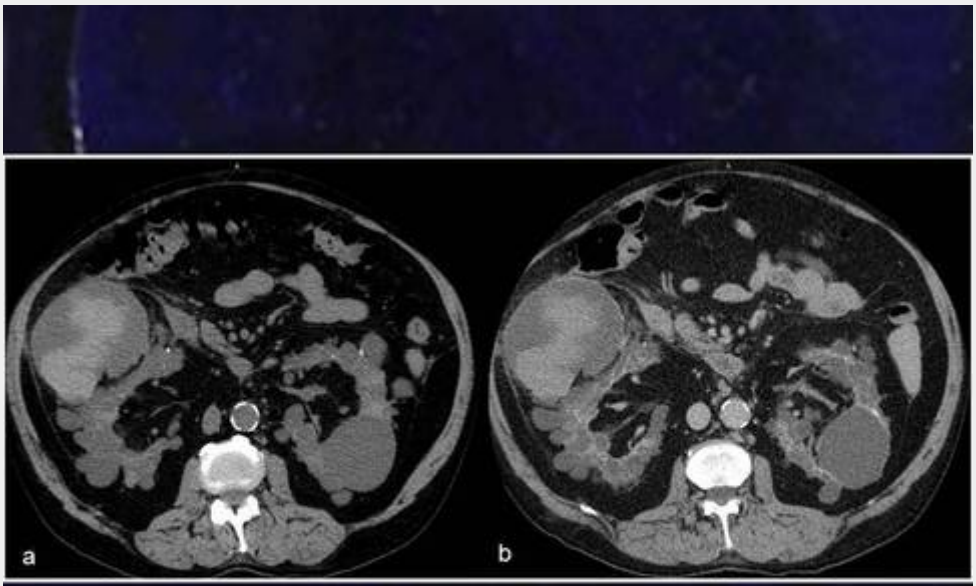

Fig. 52- Complicated renal cyst

a) and **b)** CT images show a right renal cyst with spontaneous hyperdense areas corresponding to haemorrhage in a patient with renal polycystic disease. Note also other non-complicated cysts distributed throughout both kidneys.

slide53.jpg

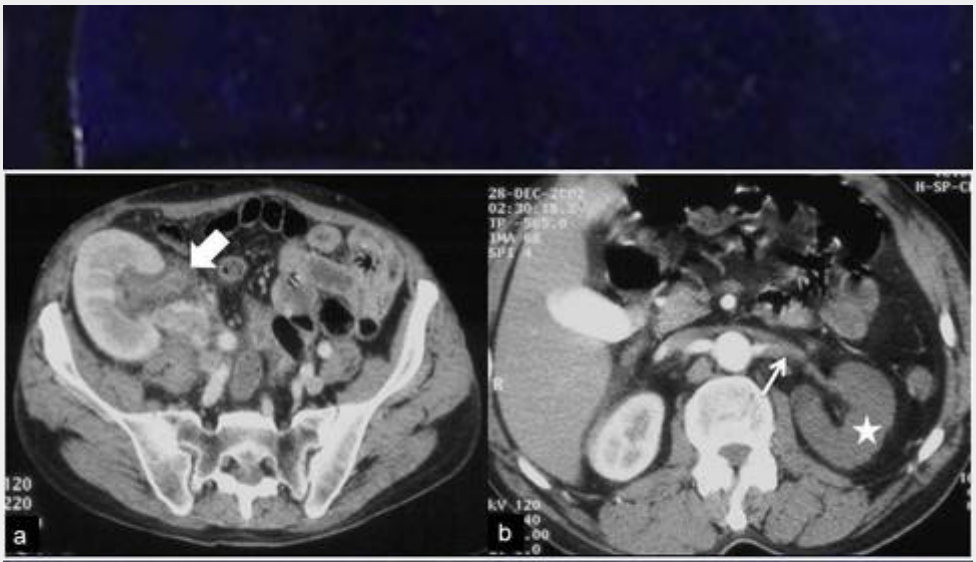

Fig. 53- Acute renal vascular conditions

a) Contrast-enhanced CT shows an enlarged, non-enhancing renal vein of a transplanted kidney, corresponding to a venous thrombosis (thick arrow); **b)** CT image depicts an arterial occlusion (thin arrow) causing left renal infarction (star).